CLASSIFICATION OF HERBICIDE-RESISTANT AND SUSCEPTIBLE KOCHIA IN SUGARBEET USING HYPERSPECTRAL AND MACHINE LEARNING TECHNIQUES

A Thesis
Submitted to the Graduate Faculty
of the
North Dakota State University
of Agriculture and Applied Science

By

Bright Mensah

In Partial Fulfillment of the Requirements
for the Degree of
MASTER OF SCIENCE

Major Program:
Agricultural and Biosystems Engineering

June 2024

Fargo, North Dakota

North Dakota State University

Graduate School

Title

CLASSIFICATION OF HERBICIDE-RESISTANT AND SUSCEPTIBLE KOCHIA IN SUGARBEET USING HYPERSPECTRAL AND MACHINE LEARNING TECHNIQUES

By

Bright Mensah

The Supervisory Committee certifies that this ***disquisition*** complies with North Dakota State University's regulations and meets the accepted standards for the degree of

MASTER OF SCIENCE

SUPERVISORY COMMITTEE:

Dr. Xin Sun
Chair

Dr. Thomas Peters

Dr. Igathinathane Cannayen

Approved:

July 5, 2024
Date

Dr. Leon Schumacher
Department Chair

ABSTRACT

The effective identification of herbicide-resistant kochia in sugarbeet fields is crucial for adopting sustainable weed management strategies. A study was conducted in a greenhouse and field to record hyperspectral data of dicamba-resistant, glyphosate-resistant, and glyphosate-susceptible kochia biotypes in sugarbeet. Hyperspectral data was captured within the wavelength of 400-1000 nm and preprocessed with Savitzky-Golay filter and Standard Normal Variate in a sequential order. Recursive feature elimination-random forest feature selection algorithm was used to select ten important wavelength bands from 224 bands. Subsequently, the features were trained on a fully connected neural network to classify dicamba-resistant, glyphosate-resistant, glyphosate-susceptible and sugarbeet. The findings revealed that a combination of hyperspectral imaging and machine learning can classify sugarbeet from herbicide-resistant kochia biotypes under varying environmental conditions. The trained deep neural network achieved multiclass classification accuracies of 93.27% in the greenhouse experiment and binary classification of 98.76% in field experiment.

ACKNOWLEDGMENTS

I would like to extend my heartfelt gratitude to the North Dakota State Board of Agricultural Research and Education, as well as the Sugarbeet Research and Education Board of Minnesota and North Dakota, for funding this project. My sincere thanks also go to the USDA National Institute of Food and Agriculture (NIFA) for their support. I am deeply grateful to my advisor, Dr. Xin Sun, for his unwavering support throughout these two years. I am thankful to Dr. Tom Peters for his assistance with the field experiment. I am grateful to Dr. Igathinathane Cannayen, for his support during my graduate studies. Special thanks to Joseph Mettler, a research specialist at the Plant Sciences Department, NDSU, for his technical assistance, and to Alexa Lystad from the Plant Sciences Department, NDSU, for her invaluable help with the field planting of sugarbeet. I would also like to acknowledge Billy Graham, Kelvin Betitame, and Mian Jilal for their significant contributions to data collection and image processing.

DEDICATION

I would like to dedicate this thesis to my family. To my mother, especially, who was there for me when I lost my father. I want to say thank you for your unwavering support, dedication, and hard work to ensure I receive the best education and training.

To my dear aunt, thank you for being the best I could ever have.

TABLE OF CONTENTS

LIST OF TABLES

LIST OF FIGURES

LIST OF ABBREVIATIONS

ANN.....Artificial Neural Network

ALS.....Acetolactate Synthase

CNN.....Convolutional Neural Network

CRD.....Complete Random Design

DL.....Deep Learning

DR.....Dicamba-resistant

EPSPS.....5-enolpyruvylshikimate-3-phosphate synthase

FLDA.....Fisher's Linear Discriminant Analysis

GR.....Glyphosate-resistant

GS.....Glyphosate-susceptible

HSI.....Hyperspectral Imaging

ML.....Machine Learning

MLP.....Multilayer Perceptron

NDSU.....North Dakota State University

NDVI.....Normalized Difference Vegetative Index

PCA.....Principal Component Analysis

PSII.....Photosystem II

RGB.....Red, Green, Blue

RF.....Random Forest

RFE.....Recursive Feature Elimination

SB.....Sugarbeet

SVM.....Support Vector Machine

SNV.....Standard Normal Variate

LIST OF APPENDIX TABLES

LIST OF APPENDIX FIGURES

1. INTRODUCTION

1.1. Background

Kochia (*Bassia scoparia (*L.*)*), a dicot weed species in the Chenopodiaceae family, is recognized as economically important in sugarbeet cultivation across the Great Plains of the United States (Geddes & Sharpe, 2022; Kumar & Jha, 2015; Nugent et al., 2018). This highly adaptable and invasive weed poses a substantial challenge to both agricultural production and environmental management. Originally native to the temperate regions of Europe, kochia was introduced into the Americas in the mid to late 1800s as an ornamental plant. It later spread worldwide thriving in arid and semi-arid environments due to dispersion by human and animal (Beckie et al., 2018; Sbatella et al., 2019).

Kochia is a bushy summer annual plant that can grow up to 72 inches tall, featuring a deep taproot system that enables it to access water from deeper soil layers. Its stems are covered with fine and soft hairs, giving the plant a grayish-green appearance. The distinctive look of kochia is further enhanced by its narrow, lance-shaped leaves and small, greenish flowers. A mature kochia plant can produce up to 30,000 seeds (Kumar & Jha, 2015; Westra et al., 2019). The seeds are dispersed by wind, water, and animals, contributing to their rapid spread and invasive nature. Its ability to thrive in drought conditions and saline soils makes it a formidable adversary. Kochia competes aggressively with crop like sugarbeet for essential resources, resulting in yield loss and declined in quality (Geddes & Sharpe, 2022; Sunil, et al., 2022).

Sugarbeet (*Beta vulgaris*), is a plant cultivated primarily for its high sucrose content, making it a valuable crop for sugar production. It is the second largest source of raw material for the sugar industry, following sugarcane (Babu & Adeyeye, 2023). The roots of the sugarbeet plant are harvested and processed to extract sucrose, which is then refined into sugar. The

economic importance of sugarbeet to the global sugar industry underscores the need to explore and implement cost-effective weed identification technologies and integrated weed management strategies that can identify and differentiate between kochia biotypes in sugarbeet crops.

The infestation of kochia in sugarbeet has been controlled by methods including mechanical weeding and herbicide application. Conventional herbicides like glyphosate and dicamba are the widely used form of weed control due to their cost-effectiveness, availability, and ease of application. Glyphosate was widely adopted for weed control because it effectively controlled a wide range of weed species. (Heap & Duke, 2018). However, the indiscriminate application of herbicide coupled with the selection pressure on a single herbicide usage led to the evolution of herbicide-resistant kochia species, creating a significant weed control challenge especially in sugarbeet (Kumar et al., 2019).

1.2. Problem statement

A study by Sbatella et al., (2019) reported kochia has developed resistance to several herbicide modes of action in addition to glyphosate, making it increasingly difficult to control with single herbicide application. This necessitates the need for innovative technologies and integrated weed management approach that can identify and differentiate between herbicide-resistant and susceptible kochia biotypes from crops. This approach will help with the development of targeted and sustainable herbicide weed control strategies (Aslan et al., 2022; Wang et al., 2019).

RGB (red, green, blue) imaging has been widely used for weed identification due to its availability and cost effectiveness. Its application which relies on features such as shape, size, and color differences between weed and crop (Esposito et al., 2021; Rai et al., 2023). However, RGB imaging is limited when utilized to differentiate between weed species with similar size,

shape, and texture specifically at the early growth stage. Its efficiency necessitates significant geometric differences between the crop and weed species (Li et al., 2021). This makes it ineffective to differentiate between herbicide-resistant and susceptible kochia species which naturally have similar features such as shape, size, texture and color (Khan et al., 2022; López-Granados, 2011).

Recently, studies have demonstrated the potential of hyperspectral imaging technology with advanced machine learning techniques to identify herbicide-resistant and susceptible weed species (Huang et al., 2018; Lee et al., 2014; Nugent et al., 2018; Scherrer et al., 2019). Hyperspectral imaging (HSI), a remote sensing and non-destructive technology, has emerged as a promising technology to capture high-resolution images of crop fields to provide information about the spatial distribution and spectral characteristics of crops and weeds (Shirzadifar et al., 2020a; Zhang et al., 2023). HSI uses the light reflectance properties between plants to differentiate them (Ram et al., 2024). The imaging system utilizes specialized advanced sensors to capture and analyze the spectral reflectance data across continuous wavelength bands in the electromagnetic spectrum (Xu et al., 2023). This allows for the detection of small variations in the unique absorption and reflectance characteristics of different plants at certain wavelengths. By analyzing the distinct spectral reflectance at different wavelengths with advanced chemometric methods, resistant and susceptible kochia biotypes can be identified and classified from crops, aiding in the development of a targeted weed control in field crops. The ability to distinguish between weed species through their spectral signatures is pivotal in precision agriculture and targeted weed management.

Therefore, this research focused on utilizing HSI to classify herbicide-resistant and susceptible kochia from sugarbeet under different environmental conditions. The experiments

were conducted in a greenhouse and field settings to capture the unique reflectance data for herbicide-resistant and susceptible kochia biotypes. The outcome of these experiments would assist with the adoption of site-specific weed management and prevent indiscriminate herbicide applications.

1.3. Objectives of the study

The objectives of this research were to (a) capture the unique spectral reflectance of herbicide-resistant and susceptible kochia biotypes before and after herbicide treatments using hyperspectral imaging; (b) develop a machine learning algorithm to distinguish between dicamba-resistant, glyphosate-resistant, and glyphosate-susceptible kochia in sugarbeet crops under greenhouse and field conditions; and (c) utilize the spectral data to assess the effectiveness of herbicides and its impact on sugarbeet.

2. LITERATURE REVIEW

2.1. Sugarbeet

Sugarbeet is one of the most economically important crops cultivated for sucrose extraction. It is the second largest source of raw material after sugarcane, contributing about 35% to the global sugar industry and 55% to the U.S. sugar industry (USDA, 2023). According to projections from the United States Department of Agriculture (2023), sugarbeet cultivation spans Minnesota, Idaho, North Dakota, Michigan, Oregon, Nebraska, California, Montana, Colorado, Wyoming, and Washington. The Red River Valley region of Minnesota and North Dakota is a major production area, with favorable climate and soil conditions for growing sugarbeet. In 2023, national sugarbeet production in the United States was estimated at around 35.23 million tons with estimated total value over $2.1 billion to domestic producers. Sugarbeet significantly impact the U.S. economy through domestic sugar production, employment in processing facilities, and economic activity in rural sugarbeet growing regions. A June 2022 report by the American Sugar Alliance found that the U.S. sugar industry, including sugarbeet, generates over $23.3 billion in economic activity annually through jobs, taxes, and economic output. Therefore, controlling weeds like kochia is crucial for maximizing yields of high-value crops like sugarbeet, which support jobs and economic activity in many rural U.S. farming communities.

2.2. Kochia

Kochia, an annual dicot weed discovered in North Dakota in 1987 , has become a significant threat to agricultural productivity for sugarbeet growers (Heap, 2024). It has been ranked as one of the top six troublesome and competitive weed species. Kochia's ability to adapt to diverse environmental conditions and its competitive nature have enabled it to invade and establish itself in many cropping systems (Sbatella et al., 2019). Moreover, human activities,

such as the movement of contaminated crop seeds, hay, and soil, along with natural dispersal methods like wind and water have facilitated the introduction and spread of kochia. Furthermore, kochia adapts to different soil types, climatic conditions, and soil disturbances, allowing it to colonize a wide range of habitats, including agricultural fields. In agricultural production, high densities of kochia can cause an average yield loss in corn (68%), soybean (52%), sugarbeet (46%), sunflower (23%), spring canola (13%), and spring oat (7%). Among these crops, sugarbeet is one of the important raw materials for sugar production (Geddes & Sharpe, 2022; Kumar & Jha, 2015). The economic loss to crops, particularly sugarbeet, is significant, highlighting the need for effective weed control methods.

2.2.1. Biology and characteristics of kochia

Kochia is an early summer species well-adapted to invading and thriving in harsh environments, such as areas with hot temperatures, significant erosion, and low water infiltration. Adverse conditions in agricultural fields, such as limited moisture and salinity, which often negatively impact crop growth and development, serves as the environment that favors the establishment of kochia populations (Geddes & Sharpe, 2022). In the fall, mature kochia plants detach at the soil surface, and tumble across the landscape, dispersing seeds with each impact in a wind-driven process that allows seeds to spread over long distances. Kochia's biology poses significant challenges due to its ability to emerge in early spring, grow rapidly, and tolerate heat, drought, and saline soil conditions. The spread of kochia, including herbicide-resistant biotypes, is further enhanced by its obligate outcrossing and tumbleweed seed dispersal mechanisms.

Kochia exhibits a unique growth pattern that enhances its competitive ability and persistence in agricultural systems. In the early stages of growth, it forms a low-growing rosette, enabling it to evade cultivation and herbicide applications. As the growing season progresses,

kochia transitions into a bushy, multi-branched plant that can reach heights of up to 2 meters, outcompeting many crops for light, water, and nutrients. The weed's C4 photosynthetic pathway, which is more efficient in terms of water and carbon use, provides a competitive advantage over C3 photosynthetic plants, particularly in hot and arid environments (Geddes & Sharpe, 2022; Kumar et al., 2019). This adaptation allows kochia to thrive in drought conditions and nutrient-poor soils, where many crop plants struggle. Furthermore, kochia has prolific seed production, where a single mature plant can produce up to 30,000 seeds, ensuring a persistent seed bank in the soil (Kumar et al., 2014). These seeds can remain viable for about two years, contributing to the long-term persistence of kochia infestations in agricultural fields. Additionally, the seeds are easily dispersed by wind, water, and agricultural machinery, facilitating the spread of the weed to new areas. Kochia's allelopathic properties, which involve releasing chemicals that inhibit the growth of other plants, further enhance its competitive ability against crops and other vegetation. These allelochemicals can disrupt various physiological processes in neighboring plants, such as germination, growth, and nutrient uptake, giving kochia a competitive edge in limited resource.

2.2.2. Herbicide-resistance in kochia

Kochia has become a problematic weed, particularly in the Great Plains states in the United States. (Kumar et al., 2021; Mosqueda et al., 2020). Kochia populations have shown resistance to PSII herbicides in Colorado, Illinois, Indiana, Iowa, Kansas, Montana, Nebraska, North Dakota, and Wyoming. Populations resistant to EPSPS inhibitors have also been identified in Colorado, Idaho, Kansas, Montana, Nebraska, Oklahoma, Oregon, and Wyoming. Furthermore, Kochia populations in Colorado, Idaho, Kansas, Montana, Nebraska, and North Dakota have demonstrated resistance to synthetic auxins. Resistance to ALS inhibitors, another type of herbicide, has been reported in Michigan, New Mexico, South Dakota, Texas, Utah,

Wisconsin, and Washington. In addition to these specific resistances, there have been reports of kochia populations in several states showing resistance to herbicides that act on multiple sites. Notably, at least one population in Kansas has exhibited resistance to all four types of herbicides mentioned above (Beckie et al., 2018; Geddes & Sharpe, 2022; Kumar & Jha, 2015; Sbatella et al., 2019). This widespread resistance underscores the adaptability of the kochia plant and the challenges it poses to effective weed control. The resistance traits of kochia make it a challenging weed to manage.

2.2.3. Kochia identification technologies

Accurate weed identification in the field is crucial for implementing site specific weed management strategies and minimizing the spread to other areas (Sunil, et al., 2022). Several methods have been employed to achieve this, each with its advantages and limitations. Kochia can be visually identified by its characteristic features, such as narrow, hairy leaves, striped stems, and compact, cylindrical seed heads that turn reddish-brown at maturity. However, visual identification can be challenging, especially in the early growth stages or when kochia is mixed with other weed species. It also requires trained personnel and can be time-consuming and labor-intensive for large-scale surveys.

RGB imaging, a cost-effective method for weed identification, utilizes the differences in physical features like shape, color, and size to distinguish weeds from crops. However, it struggles to differentiate between spatially similar crops and weeds, especially during the early growth stage, a critical period for effective weed control (Graham-Ram et al., 2023). Recently, remote sensing technologies, particularly multispectral and hyperspectral imaging, have shown great potential for the identification and mapping of kochia weed. These techniques exploit the unique spectral signatures of kochia at different growth stages and its reflectance properties

across multiple wavelengths of the electromagnetic spectrum. Multispectral imaging, which captures data in a few broad spectral bands (e.g., red, green, blue, and near infrared), can provide valuable information for distinguishing kochia from other vegetation based on its spectral reflectance patterns. However, the limited spectral resolution may not be sufficient for accurate discrimination between kochia and spectrally similar species.

HSI captures data in hundreds or even thousands of narrow, contiguous spectral bands, providing a detailed spectral signature for each pixel in the image. This high spectral resolution allows for the detection of subtle differences in the spectral responses of kochia plants, enabling early detection and accurate mapping of infestations, even at the seedling stage (Khan et al., 2022). Advanced image processing and machine learning techniques have been integrated with hyperspectral data to improve the accuracy of kochia identification and classification. These algorithms can learn the complex patterns and relationships between spectral signatures and plant species, facilitating automated and large-scale mapping of kochia distribution in the field. Accurate weed identification and classification is essential for mitigating the spread and impact of kochia, particularly herbicide-resistant species.

2.3. Hyperspectral imaging technology

Hyperspectral imaging (HSI), also known as imaging spectroscopy, is an advanced remote sensing technique that captures information from the visible near infrared and short-wave infrared region of the electromagnetic spectrum (Figure 1). This technology has found widespread applications in various fields, including soil and crop monitoring, plant diseases detection, and weed identification (Graham-Ram et. al, 2023).

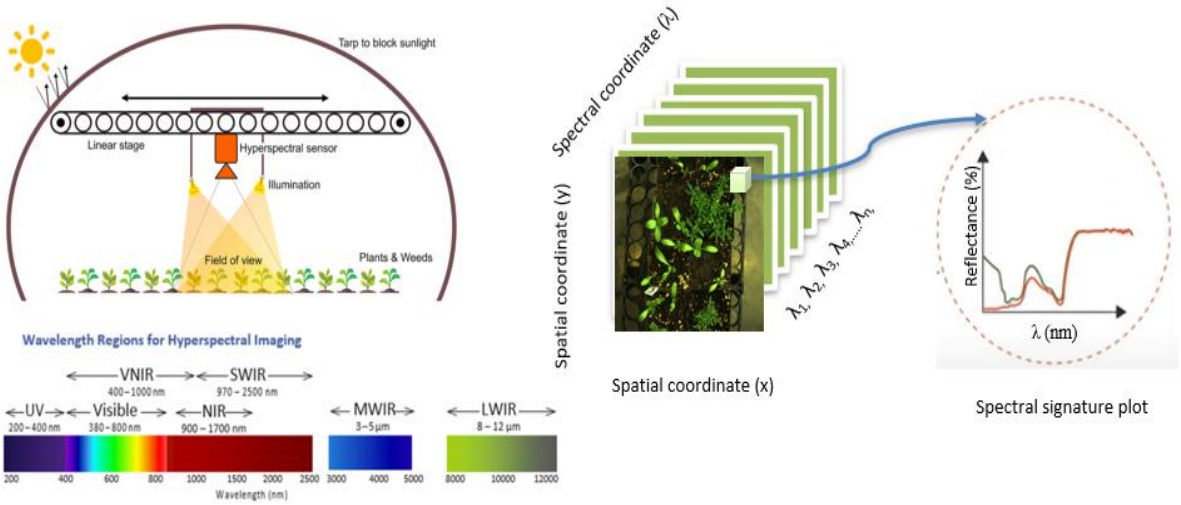

Figure 1. Illustration of hyperspectral imaging technology for weed and crop identification under field conditions.

Moreover, in precision agriculture, it has shown promise in monitoring spatial-temporal variations of crop morphological and physiological status, supporting precision weed identification and management (Rai et al., 2023). HSI is particularly useful for weed identification in agricultural fields due to its ability to capture detailed spectral information. HSI uses the difference in spectral reflectance between weeds and crops to identify weeds in crop allowing for the application of site-specific weed management. The key components of the imaging system typically include a spectrometer, a detector array, and an imaging optics system. The spectrometer disperses the incoming light into its constituent wavelengths, while the detector array captures the spectral information for each spatial location within the scene. The imaging optics system projects the target scene onto the detector array, which then measures the amount of light that is reflected or emitted from the plants surface (Mishra et al., 2020; Paoletti et al., 2019). The sensor measures the unique reflectance also called spectral signature for each pixel in an image plane by raster-scanning across hundreds of wavelength bands to generate a three-dimensional (3D) datacube (x, y, λ). The 3D datacube contains information about the

intensity of light reflected at a specific wavelength (λ) at a spatial location (x, y) (Pott et al., 2020; Chang et al., 2020; Istiak et al., 2023).

In weed identification studies, HSI is utilized to acquire data across multiple narrow and contiguous spectral bands, typically ranging from visible infrared range (400-1000 nm) and near-infrared range (900-1700 nm) of the electromagnetic spectrum (Wieme et al., 2022). The sensor captures high-resolution spectral information for each pixel within an image, enabling the identification and differentiation of objects based on their unique spectral characteristics. These spectral signatures provide detailed information about the chemical and physiological properties of both crops and weeds, allowing for discrimination between weed species and crop plants.

Several studies have utilized hyperspectral sensors to distinguish weeds from crops in various environments (Diao et al., 2023; Graham Ram et al., 2023; Lauwers et al., 2020, 2022). Huang et al. (2018) used hyperspectral imaging to differentiate between glyphosate-resistant and glyphosate-susceptible Italian ryegrass (*Lolium perenne*), achieving a classification accuracy of 75% to 80%. Similarly, Nugent et al. (2018) utilized hyperspectral imaging to identify dicamba-susceptible, glyphosate-resistant, and glyphosate-susceptible kochia with accuracies of 80%, 67%, and 76%, respectively. Scherrer et al. (2019) employed hyperspectral imaging and neural networks to classify herbicide-resistant weeds at different growth stages, with accuracies ranging from 77% to 99%. These studies underscore the significant potential of hyperspectral imaging in identifying and discriminating herbicide-resistant and susceptible weeds for effective weed management.

Hyperspectral sensors capture over hundreds contiguous spectral bands, providing a detailed and continuous spectral signature for each pixel in the image. Because each plant species has a unique spectral signature, determined by factors such as chlorophyll content, cell

structure, and water content. When they are exposed to light radiation, the difference in chemical composition results in variation in the absorption and reflectance of light at specific wavelengths, which can be extracted and processed for identification and classification of plant species. Compared to imaging technology such as multispectral and RGB (red, green, blue) imaging, it captures data in a few broad spectral bands typically between 3-10 bands or channels.

2.3.1. Weed identification process using hyperspectral imaging

The traditional approach to hyperspectral weed identification follows a sequential process. First, a hyperspectral image or spectra data is captured, which is then calibrated using white and dark references. This is succeeded by segmentation, spectral preprocessing, and feature selection. Subsequently, the data is transformed, converting a 3-dimensional image into a 2-dimensional table filled with reflectance values that serve as input for subsequent analysis. This conventional preprocessing method for hyperspectral data is commonly used in numerous agricultural weed identification studies (Ram et al., 2024).

A hyperspectral sensor is normally mounted on a ground or unmanned aerial platform to acquire spectral data across hundreds of contiguous wavelength bands in the visible and near-infrared regions of the electromagnetic spectrum. The acquired hyperspectral data is processed and analyzed to identify the spectral signatures of different crop and weed species. The sensor captures a vast amount of data, resulting in redundancy. To tackle this, we perform feature selection to identify and choose the most important features, ensuring they provide distinguishable information for classification. This involves the application of advanced image processing and machine learning algorithms to classify hyperspectral data. These algorithms compare the spectral signatures of each pixel in the image with the spectral library, enabling the identification and mapping of different crops and weeds species. Subsequently, the classified

hyperspectral data provides spatial information about the distribution and density of weeds in the agricultural field. This information is then used for targeted and site-specific weed management strategies, such as selective herbicide application or mechanical removal, reducing the overall use of chemical inputs and minimizing environmental impact.

2.3.2. Weed classification using machine learning techniques

Weed classification techniques, a crucial aspect of hyperspectral imaging, employ several approaches for weed identification. These include spectral feature extraction, machine learning (ML), and deep learning algorithms (DL) for classification. The unique spectral responses of weeds and desirable plants can be distinguished using spectral reflectance properties, absorption features, and vegetation indices. A fundamental step in hyperspectral weed identification is extracting relevant spectral features from the acquired data. These features can be specific wavelengths or spectral bands sensitive to the chemical composition, pigments, or structural properties of plant species. For instance, the red and near-infrared regions of the spectrum are particularly useful for detecting differences in chlorophyll content and vegetation health, aiding in differentiating weeds from crops. Additionally, spectral absorption features associated with pigments like chlorophyll and carotenoids can be exploited to characterize plant species (Li et al., 2021). These features appear as distinct patterns or spectral signatures, enabling the identification of specific plant types.

Vegetation indices are mathematical combinations of spectral bands created to highlight specific features of vegetation while minimizing the influence of factors like soil background or atmospheric effects. In hyperspectral weed identification, commonly used vegetation indices include the Normalized Difference Vegetation Index (NDVI). This index offers valuable insights into plant health, biomass, and photosynthetic activity, which help differentiate weeds from

crops (Vélez et. al., 2023). Classification algorithms are employed to identify and map the distribution of weeds after extracting the relevant spectral features and vegetation indices. Classification algorithms used in hyperspectral weed identification include supervised classification, unsupervised classification, and spectral matching techniques.

Supervised classification involves training the algorithm with a set of known spectral signatures or ground-truth data for different plant species, including weeds and crops. The algorithm learns to recognize these patterns and can then classify new hyperspectral data based on the trained model. In contrast, the unsupervised classification algorithm, such as k-means clustering algorithm automatically groups pixels in the hyperspectral data based on their spectral similarities, without prior knowledge of the plant species. This approach can be useful for exploratory analysis or when ground-truth data is limited. Spectral matching techniques involve comparing the spectral signatures of each pixel in the hyperspectral data with a reference spectral library of known plant species. The closest match determines the classification of that pixel as a specific weed or crop species.

The application of deep learning, specifically 3D convolutional neural network (3D-CNN) has gained significant popularity in hyperspectral weed identification in recent years due to their ability to handle complex and high-dimensional data. Approaches such as artificial neural networks, support vector machines (SVM), random forests (RF), and DL algorithms have been applied to hyperspectral data for accurate weed classification. These machine learning models can be trained on labeled hyperspectral data, allowing them to learn the intricate spectral patterns and relationships between different plant species. Once trained, the models can effectively classify new hyperspectral data, identifying weeds and crops with high accuracy. Advanced techniques like transfer learning and data augmentation can help overcome challenges such as

limited training data or spectral variability caused by environmental factors. By combining spectral feature extraction, vegetation indices, classification algorithms, and machine learning techniques, researchers and practitioners can leverage the rich information provided by hyperspectral imaging to develop robust and accurate weed identification systems, enabling more targeted and sustainable weed management practices in agriculture (Li et. al., 2024).

3. MATERIALS AND METHODS

3.1. Experiment site and data collection

This research, conducted from January 2023 to July 2023, comprised two distinct experiments. Each experiment involved acquiring hyperspectral data for sugarbeet and kochia biotypes, both before and after the application of herbicides. The first experiment took place in a controlled greenhouse environment, while the subsequent one was carried out in a sugarbeet field.

3.1.1. Greenhouse experiment setup for image acquisition

The experiment was conducted in January 2023 at Plant Science Department greenhouse at North Dakota State University (NDSU), North Dakota, USA. Sugarbeet hybrid (BTS 8927 Beta seed, KWS Seeds, Minneapolis, MN, 2022) seeds and three different kochia biotypes [(Kochia 2015 #2 (dicamba-resistant), NW22 2021 (glyphosate-resistant), and 2019 BASF (glyphosate-susceptible))] were sourced from the Plant Science Department at NDSU. A Kindred silty clay loamy soil obtained from NDSU Casselton, ND Seed Farm was autoclaved and mixed with PRO-MIX general purpose greenhouse media (Premier Horticulture, Inc., Quakertown, PA). An equal proportion was added to the 10 × 10 × 9 cm greenhouse pot to a depth of 7.5 cm. Multiple seeds were planted in pots, covered with soil, and gently pressed to maintain uniform soil contact. The samples were watered regularly to keep the soil moist, ensuring healthy plant growth and germination. Solar vapor lamps were used as a supplement light source to provide energy and generate germination conditions. The temperature was maintained at 10ºC, throughout the experiment. Kochia was thinned to 5 plants per pot, and sugarbeet was thinned to 1 plant per pot to allow for effective image collection approximately 10 days after seed emergence (Figure 3).

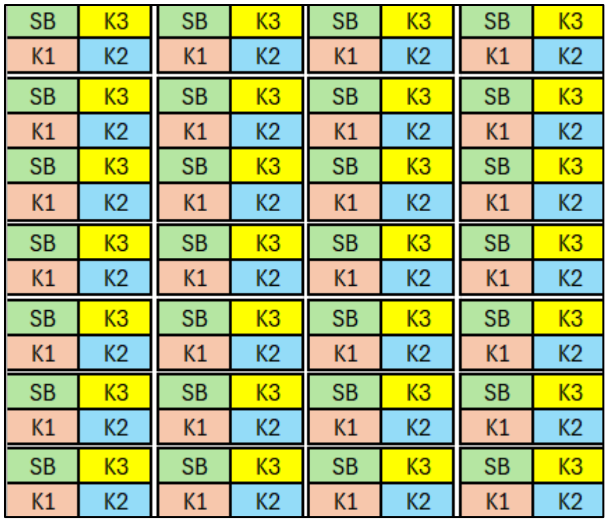

Figure 2. Experimental design in the greenhouse for kochia and Sugarbeet data collection, SB-sugarbeet, K1-kochia (dicamba-resistant), K2-kochia (glyphosate-resistant), and K3-kochia(glyphosate-susceptible).

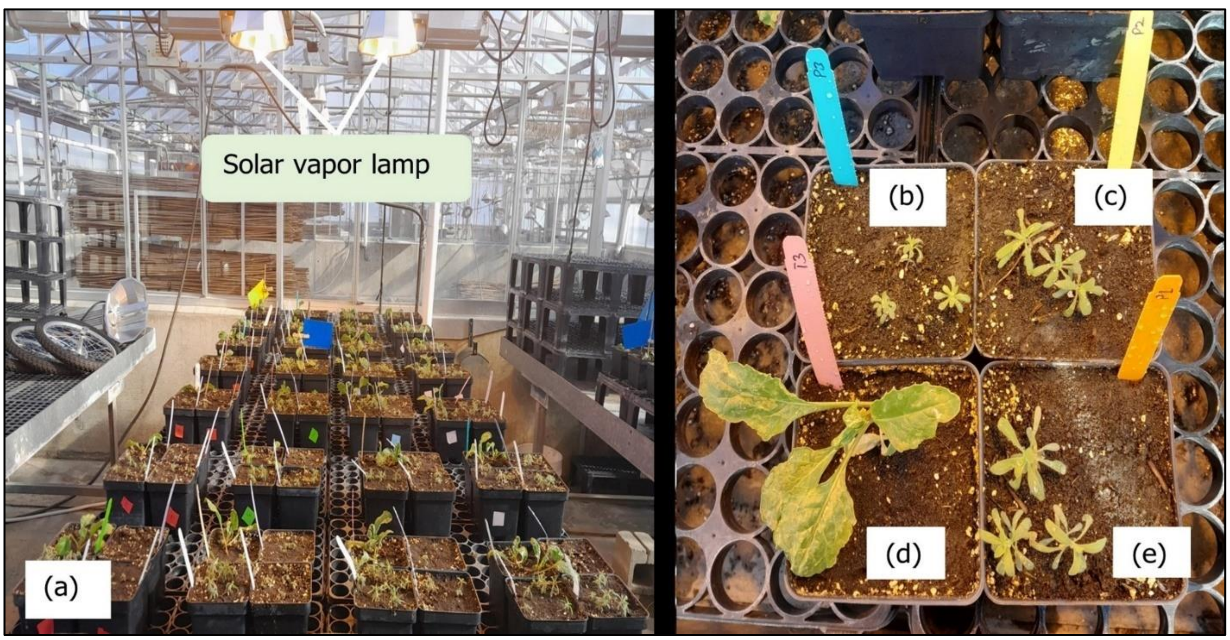

Figure 3. Greenhouse experiment design (left) indicating sugarbeet and kochia biotypes 3 weeks after planting, a) complete random design (CRD), b) glyphosate-susceptible (GS) kochia, c) glyphosate-resistant (GR) kochia, d) sugarbeet, and e) dicamba-resistant (DR) kochia.

3.1.2. Herbicide treatments applied to sugarbeet and kochia in greenhouse and field

The herbicide treatments utilized in the greenhouse experiment were trisulfuron-methyl, fluroxypyr-ester, florpyrauxifen-benzyl, glyphosate, glyphosate + florpyrauxifen-benzyl, and

acifluorfen (Appendix A). These herbicides are used by sugarbeet growers to suppress broad-leaved weeds and kochia in sugarbeet fields in North Dakota. The herbicide treatments were applied to sugarbeet and kochia biotypes in the greenhouse experiment four weeks after planting, or when sugarbeet was at 4 to 5 leaf stage and approximately 9 cm in height. Likewise, kochia biotypes were at 5 to 6 leaf stage and 4 cm in height. Herbicides were applied using a moving-nozzle cabinet sprayer (Generation III, DeVries Manufacturing, Hollandale, MN) calibrated to deliver 159 Lha^{-1} of spray solution at a pressure of 276 kPa, moving at a speed of 2.6 kmh^{-1}, at a boom height of 33 cm. These conditions ensured that the herbicide was effectively delivered to the target plants while minimizing the risk of drift or excessive herbicide application. The greenhouse environment was carefully monitored during the herbicide spraying process to ensure optimal conditions for herbicide application. The air temperature in the greenhouse was 25 ºC, with a soil temperature of 28 ºC, relative humidity of 22%, and cloud cover of 20%. Figure 4 illustrates the effect of herbicide treatment on the kochia biotypes during a greenhouse experiment.

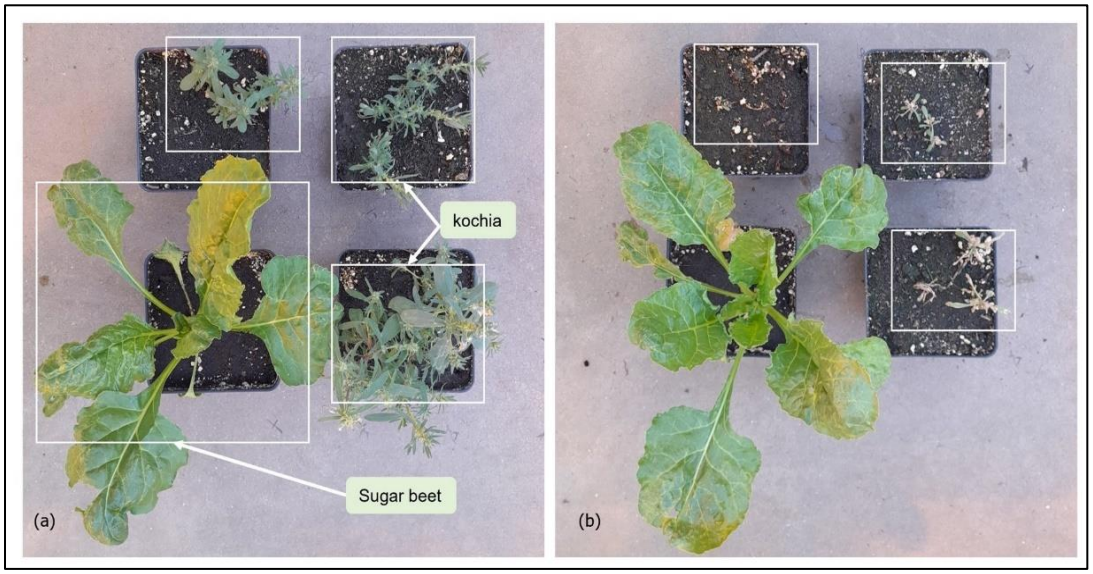

Figure 4. Illustration of herbicide effects after application to sugarbeet and kochia during greenhouse experiment, a) plants before treatment, and b) kochia and sugarbeet after treatment.

3.1.3. Field experiment

The experiment was conducted in a sugarbeet field at the Casselton Agronomy Seed Research Farm, North Dakota, USA (Figure 5). The experimental unit was divided into 28 subplots, each measuring 4.8 m × 1.15 m (5.52 m^2) and 1.6 m buffer between subplots.

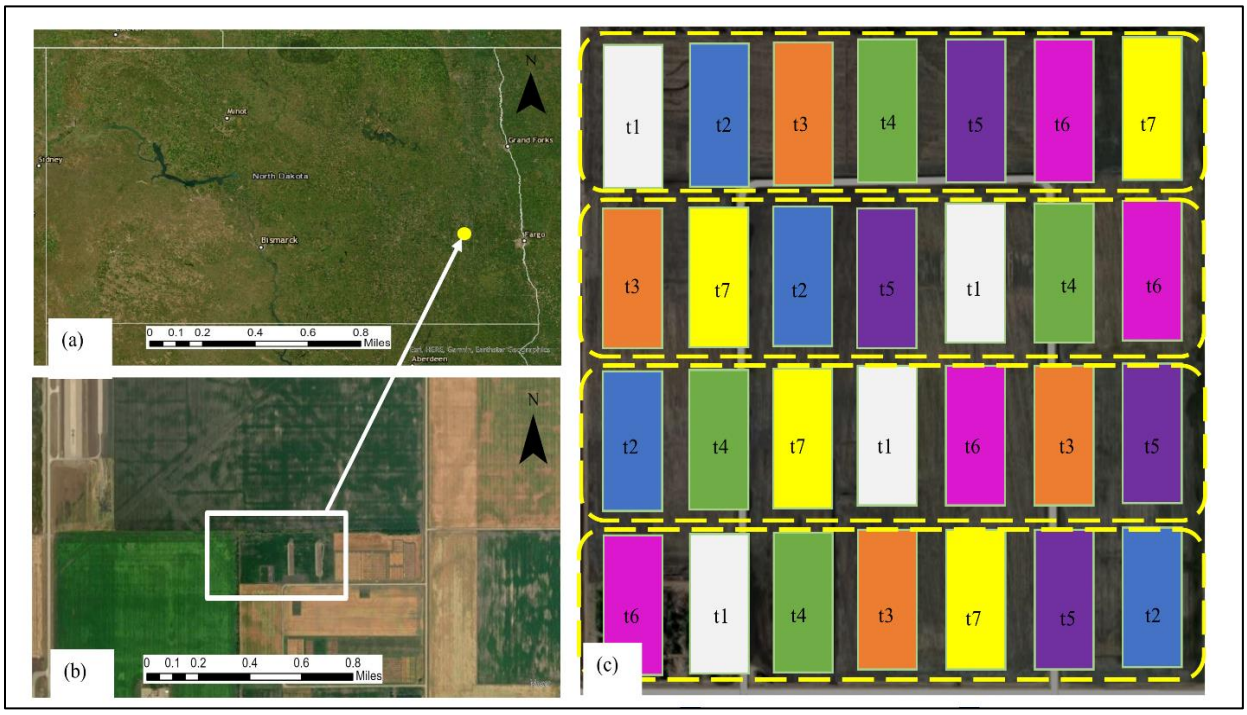

Figure 5. Plot layout for herbicide application and data collection in the field a) Agronomy Seed Farm, Casselton, North Dakota b) NDSU Plant Science block c) plot layout for herbicide (Untreated plants (t1), trisulfuron-methyl (t2), fluroxypyr-ester (t3), florpyrauxifen-benzyl (t4), glyphosate (t5) glyphosate + florpyrauxifen-benzyl (t6), and acifluorfen (t7).

3.1.3.1. Kochia preparation for field planting

Soil was collected from the experiment area and transferred to the Agricultural Experiment Station Greenhouse at NDSU for autoclaving. The treated soil was mixed (1:1) with PRO-MIX potting soil to germinate the kochia. An equal proportion was added to 10 × 10 × 9 cm greenhouse pot to a depth of 7.5 cm. Multiple seeds were planted in the pots, covered with soil, and gently pressed to maintain uniform soil contact. Watering was done regularly to keep the soil moist, ensuring good germination. The kochia was thinned to 5 plants per pot for

effective image collection. The plants were then transferred to the field experiment site for planting.

3.1.3.2. Field planting of sugarbeet and kochia

Sugarbeet variety CR 793 (Crystal Sugarbeet, Moorhead, MN) was planted on June 2, 2023, at a seeding rate of approximately 60,500 seeds per acre to a planting depth of approximately 4 cm, with 3 crop rows per subplot spaced approximately 56 cm apart. Greenhouse grown GR kochia biotypes were transplanted into the field on June 24. Poor emergence of DR and GS kochia prevented their used in the field experiment. Kochia seedlings were planted inter row throughout the experiment area to ensure a diverse mix of sugarbeet and kochia. Water was delivered to the sugarbeet and kochia using a truck-mounted water tank and a hand-held sprinkler with manual rate control until they were established. The herbicide treatments utilized in the field experiment are trisulfuron-methyl, fluroxypyr-ester, lorpyrauxifen-benzyl, glyphosate, glyphosate + florpyrauxifen-benzyl, and acifluorfen (Appendix B). Herbicide treatments were applied in the field with a hand-held sprayer at a pressure of 276 kPa, at a rate of 140 Lha^{-1}, in conditions of 13ºC air temperature, 18ºC soil temperature, 76% humidity, wind velocity of 2.4 kmh-1, and about 15 % cloud cover.

3.2. Hyperspectral weed identification workflow for greenhouse and field experiments

The procedures for the weed identification workflow involved the collection of hyperspectral images of both sugarbeet and the kochia biotype. These images were then preprocessed to extract the most significant spectral data. The preprocessing stage involved several steps, including raw image calibration using white and dark reference image, segmentation to remove background, signal scatter correction, and the selection of sensitive wavelength bands for machine learning and classification. Preprocessing of hyperspectral data is

crucial as it enhances the quality of spectral data. It does so by extracting significant spectral information and ensuring that the data is in a format for machine learning. The entire weed identification workflow is represented in Figure 6.

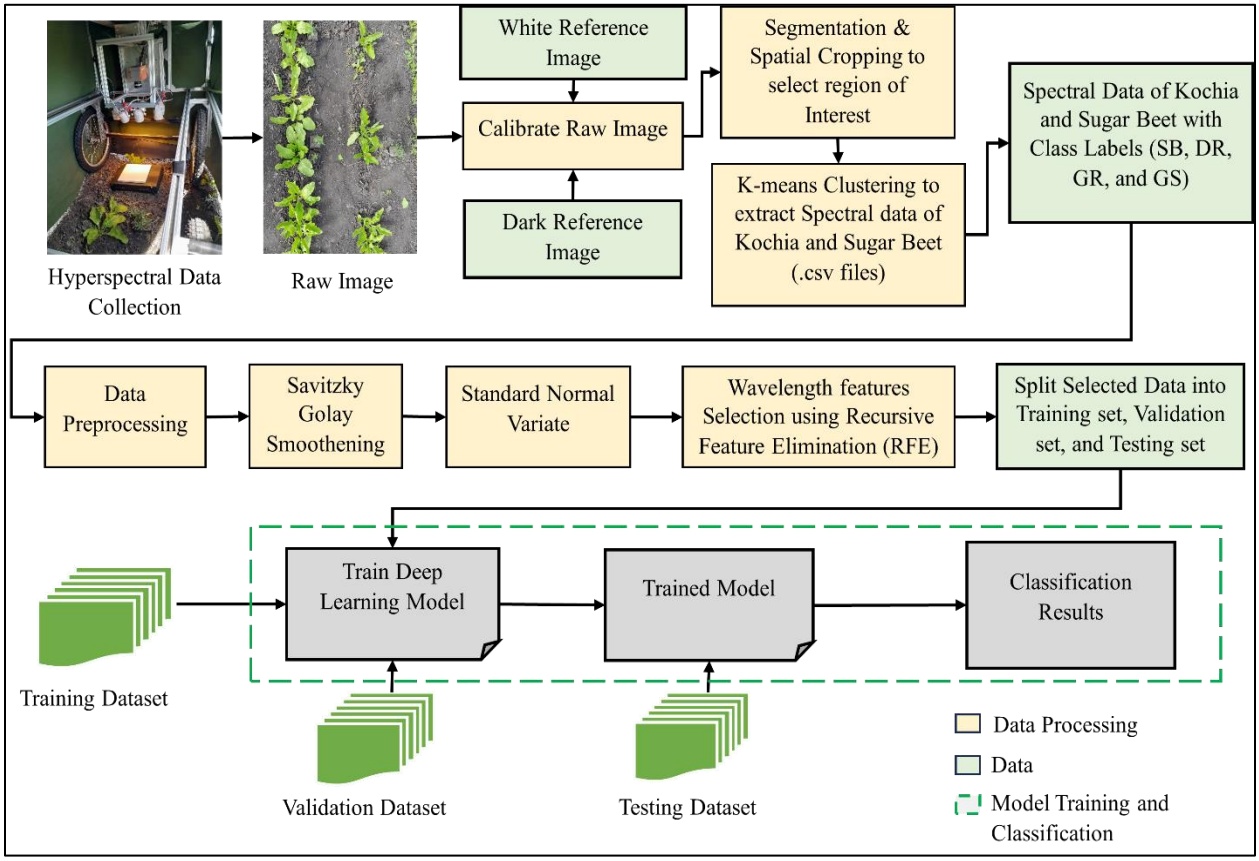

Figure 6. Workflow for hyperspectral weed classification of sugarbeet and kochia biotypes in greenhouse and field experiment.

3.2.1. Data collection for sugarbeet and kochia in greenhouse and field

Sugarbeet and kochia were imaged using a line scan sensor, Specim FX 10 hyperspectral imaging system (Finland, Oulu), with a spectral range of 393 to 1003 nm, with 224 wavelength bands and 5 nm spectral resolution. The sensor was mounted on an in-house fabricated scanning platform approximately 15 cm above the plants (Figure 7a). The scanning platform included 7 halogen lamps (50 watts) positioned at a 30º angle from the vertical plane to serve as the illumination source and a white Teflon tile served as a reference to calibrate the light intensity.

The camera's exposure time was set to 8 msec, while the position speed of the linear stage was adjusted to 10.1 mm s^{-1}. A white Teflon tile measuring 24 cm × 24 cm × 1 cm with about 99% reflectivity was placed beneath the hyperspectral camera to capture the white reference image. The camera lens was covered to capture the dark reference image for raw image calibration. The scanning platform steadily moved across the plants at 5.0 mm s^{-1}, capturing high-resolution images. The kochia and sugarbeet were carefully scanned to ensure accuracy and eliminate occlusion from adjacent plant leaves. The setting of the camera's exposure time and position speed ensured that the data obtained was accurate.

Figure 7. Field data collection (a) hyperspectral sensor mounted on a scanning platform for data collection of raw, white reference and dark reference image (b) raw RGB image.

Hyperspectral image data were captured for weed identification and classification. Hyperspectral data were collected during the vegetative growth stage, specifically at the 6-leaf stage for sugarbeet and the 5-leaf stage for kochia biotypes. The raw images were calibrated, and the corrected intensity values were then preprocessed to remove noise and redundant information

captured during the image acquisition process. Table 1 details the specifications of the hyperspectral sensors whereas Tables 2 provides the number of images captured in the greenhouse and field for weed identification.

Table 1. Specification of hyperspectral imaging system utilized to capture images.

Parameter name	Value
Hyperspectral sensor	Specim FX10
Image size	1340 × 1024 pixels
Wavelength	393 – 1003 nm
Illumination	454 mA (50W) at 110 – 130V halogen lamps
Wavelength bands	224

Table 2. Number of raw images captured by the hyperspectral sensor.

Sample	Number of images captured by the sensor		Illumination Source
	Greenhouse	Field	
Sugarbeet	28	37	Direct halogen lamp
DR	28	37	Direct halogen lamp
GR	28	-	Direct halogen lamp
GS	28	-	Direct halogen lamp

Note: DR-dicamba-resistant kochia, GR-glyphosate-resistant kochia, and GS-glyphosate-susceptible kochia.

3.2.2. Calibration of hyperspectral image

Image calibration in close-range hyperspectral imaging of plants is an essential process to help extract useful information from the acquired image. The geometry of plant leaves can cause scattering and multiple reflections of incoming light sources, resulting in irregular patterns that may obscure the true spectral reflectance. As a result, image calibration serves to correct these illumination variations, allowing for more accurate analysis and interpretation data. The raw intensity values from sensor were converted to reflectance values using Equation 1.

$$R_{\text{cal}} = \frac{R_{\text{raw}} - R_{\text{dark}}}{R_{\text{white}} - R_{\text{dark}}} \quad (1)$$

where R_{raw} = the original hyperspectral image

R_{white} = the white reference image collected with Teflon board with 99% reflectance

R_{dark} = the dark reference image

R_{cal} = the corrected reflectance image

The use of pixel calibration allows for the correction of both spatial and wavelength-dependent variations caused by non-uniform illumination differences in sensor sensitivity. This combination is recommended for accurate hyperspectral image transformation from instrument values to reflectance values (Burger & Geladi, 2005, 2006). An image segmentation algorithm was used after converting the raw hyperspectral image to reflectance value to separate the pixels belonging to the plants from those belonging to the background. This was achieved by using K-means clustering technique which helped to select the region of interest (sugarbeet and kochia biotypes) from the background.

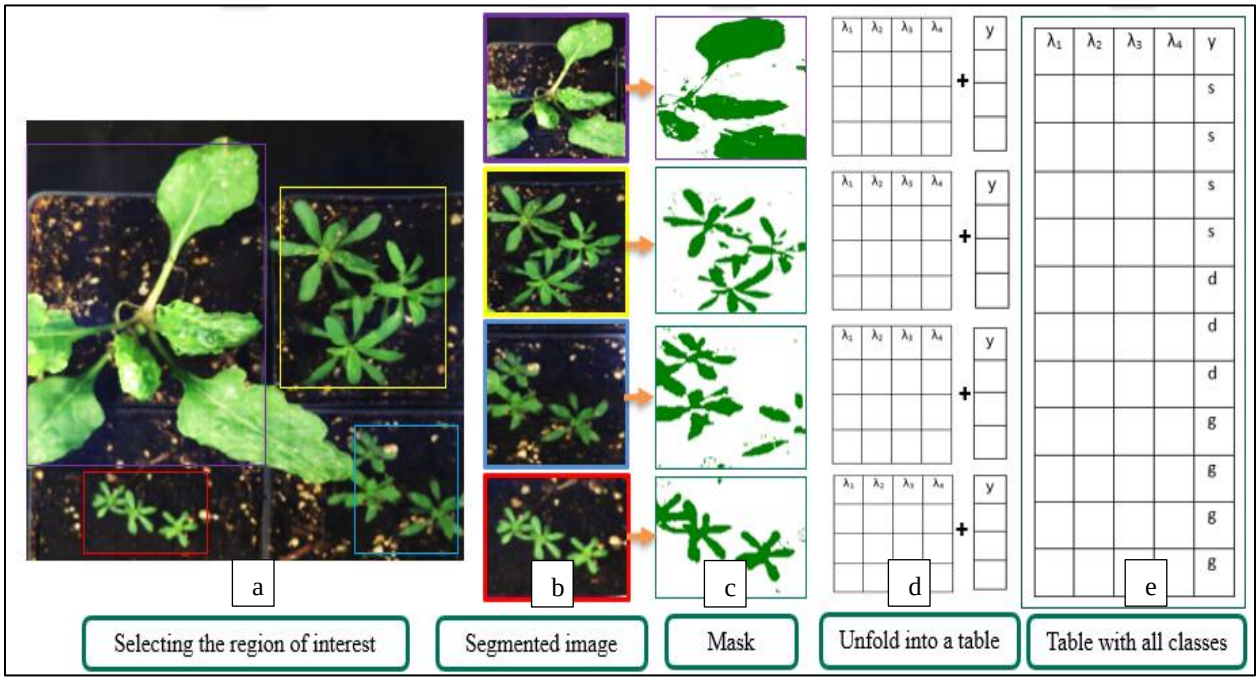

Figure 8. Illustration of hyperspectral image preprocessing of greenhouse and field images to extract spectral values of Sugarbeet and kochia biotypes for machine learning and classification.

K-means clustering algorithm is one of the popular methods that groups image pixels into k-clusters according to the similarity of the spectral features (De Juan et al., 2014; Piqueras et al., 2011). The algorithm groups pixels into homogeneous clusters, distinguishing between background and plant areas. After identifying the clusters that correspond to the plant (either kochia or sugarbeet), a mask is created and applied to the segmented image to isolate the plant, effectively removing the background (Figure 8c). The spectral values of the masked image are then extracted by unfolding the image, which converts the multidimensional array into a two-dimensional table. This process removes the spatial resolution while retaining the full spectral resolution of 224 bands (Figures 8d & 8e). Finally, the true class label is appended to each table entry as a reference for machine learning training and testing. The data was saved in a standard comma-separated values (.csv) format to facilitate data processing.

3.2.3. Hyperspectral data preprocessing methods for machine learning

Hyperspectral data contain enormous amounts of information, but the quality of the raw measurements can be affected by high signal noise levels, instrumentation variations, and environmental factors like variation in solar radiation which can have an impact on the data interpretation. Therefore, to correct for these undesirable effects, spectra preprocessing techniques, namely the Savitzky-Golay (SG) smoothing method and standard normal variation (SNV) were used in a forward manner to correct these signal defects and eliminate any possible high-frequency signal noise. Preprocessing filters, SG and SNV were found to generate the best discriminating results, like results by Shirzadifar et al., (2018).

SG smoothening method (Savitzky & Golay, 1951) was performed on the raw data to isolate important spectra features that may be partially masked by noise from scanning instruments. Subsequently, SNV techniques were used to help balance instrumentation variations

and remove the effect of scattering from the spectral data, leaving only the absorption characteristic. SNV scatter correction process involves two primary steps. First, it centers each spectrum denoted by S_i, by subtracting the mean $\overline{S_i}$, from each spectrum. Second, it normalizes each mean-centered spectrum by dividing it by its standard S_{std} as shown in Equation 2.

$$S_{snv} = \frac{S_i - \overline{S_i}}{S_{std}} \quad (2)$$

where S_i = the spectral data

S_{std} = the standard deviation of the spectral data

$\overline{S_i}$ = the mean of spectral data

S_{snv} = the corrected spectral data

Removing the mean value of each spectrum and dividing the result by the standard deviation compensates for these biases, normalizes the spectra, and adjusts the scale, effectively eliminating the influence of additive effects. After the SNV transformation, each spectrum will have a mean of 0 and a standard deviation of 1, resulting in all spectra being of equal intensity for machine learning. SNV is a popular chemometrics spectral scattering technique widely used in hyperspectral imaging technology to improve the quality of the spectral data, especially when used for predictive models (Mishra et al., 2020). In this study, SNV was opted for instead of multiplicative scatter correction (MSC) because SNV does not require any reference measurements compared to MSC. Additionally, SNV does not rely on additional sensor measurements for signal correction (De Juan et al., 2014), but focuses on correcting additive effects, which can introduce systematic biases and complicate accurate comparison and analysis of different spectra. The SG smoothing method and SNV are essential when it comes to hyperspectral data analysis, as the techniques significantly enhance the quality and reliability of data for machine learning (Shirzadifar et al., 2018).

3.2.4. Wavelength bands selection using recursive feature elimination

The presence of non-informative wavelength features can introduce bias and significantly influence the performance of the predictive model. It can potentially affect the overall accuracy of the prediction results. Therefore, removing any redundant and non-informative features has the potential to improve the model's performance and subsequent data analysis. The process known as feature selection or extraction is designed to decrease the number of input features and simplify the training of the predictive model. This has the benefit of enhancing prediction accuracy, speeding up the prediction process, and lowering the computational power and resource. Therefore, by limiting the features to only the most important wavelengths, the model becomes more efficient and robust (Kanthi et al., 2020). This is especially true when working with large datasets or complex models, where it is important to save computational resources by picking out a relevant subset of features.

The research developed a recursive feature elimination-random forest (RFE-RF) algorithm to select ten informative wavelength bands. The feature selection process is illustrated in Figure 9. RFE is a wrapper technique that works by recursively removing less important wavelength bands iteratively, and then generate new models with the remaining subset of features and evaluate the predictive ability based on performance matrices, e.g., accuracy. The selection process used an equal number of preprocessed spectral data (pixels values) randomly selected from both greenhouse and field data. Selecting balanced samples helps to address the issues related to imbalanced datasets. Imbalanced datasets can introduce biases during the feature selection process and potentially impact the accuracy of the model's classification results. The feature selection process begins by fitting all the 224 wavelength bands as features into the random forest (RF) classifier as the base estimator to rank the features.

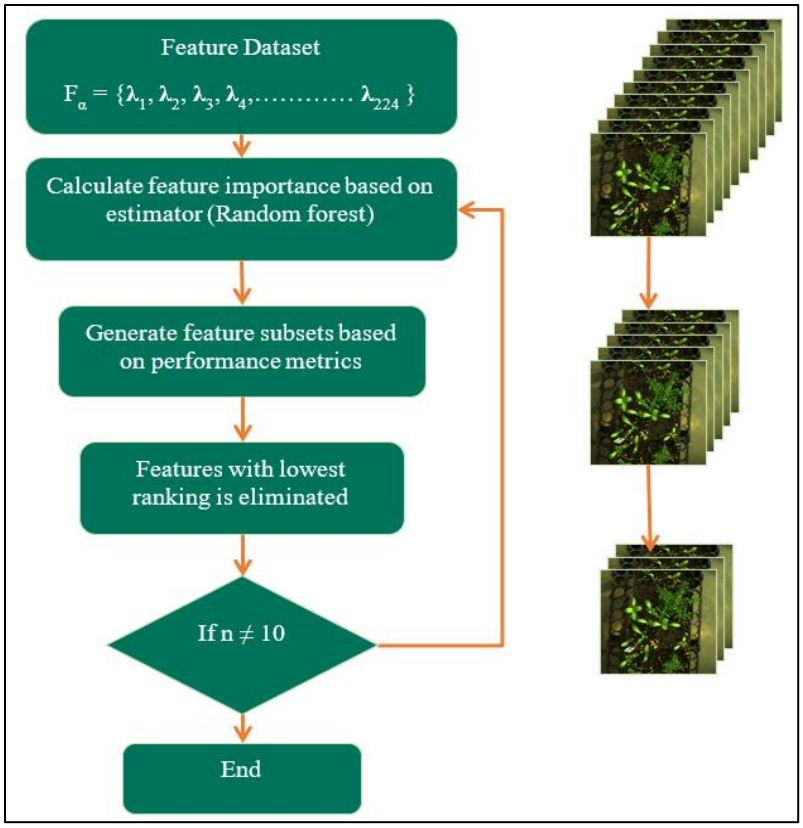

Figure 9. Illustration of wavelength features selection process using recursive feature elimination method to select 10 important wavelength features to classify Sugarbeet from kochia biotypes.

The RF classifier sequentially eliminates the least significant wavelength bands that exhibit lower predictive performance. The iterative process continues until the desired number of features (n = 10) is reached and there is no significant improvement in the performance metric, such as the classification accuracy. The benefit of this method is its ability to independently assess and assign rankings or scores to wavelength features, irrespective of the learning algorithm employed. Therefore, RFE-RF facilitates the rapid identification of potentially informative features based on their intrinsic discriminating characteristics. The selected 10 wavelength features were randomly split into two groups, where 70% of the data was used for training and validation of the deep neural network and the remaining 30% used as testing

datasets for evaluating the performance. The total number of training and testing samples is presented in Table 3 and Table 4.

Table 3. Selected spectra data for each class from greenhouse data for machine learning.

Class	Training samples (pixels)	Testing samples (pixels)	Total samples (pixels)
Sugarbeet	35000	15000	50000
DR	35000	15000	50000
GR	35000	15000	50000
GS	35000	15000	50000

Note: DR-dicamba-resistant kochia, GR-glyphosate-resistant kochia, and GS-glyphosate-susceptible kochia.

Table 4. Selected spectra data for each class from field data for machine learning.

Class	Training samples (pixels)	Testing samples (pixels)	Total samples (pixels)
Sugarbeet	35000	15000	50000
GR	35000	15000	50000

Note: GR-glyphosate-resistant kochia.

3.2.5. Machine learning architecture and classification metrics

A fully connected neural network (FCNN) was developed and trained on the given dataset using a backpropagation method. The network's architecture consists of an input layer, two hidden layers, and an output layer (Figure 10). The input layer (feature input) has an input size that matches the dimensionality of the input data, while the output layer (class output) has a size that corresponds to the number of classes in the classification task. Between the input layer and the first hidden layer, a batch normalization layer is added to stabilize and accelerate the training and the learning process by normalizing input weights. The first hidden layer follows, performing a linear transformation and then applying the Rectified Linear Unit (ReLU) activation function. Rectified Linear Unit (ReLU) activation function is utilized, which helps the model generalize better to the inputs and differentiate between output classes more effectively.

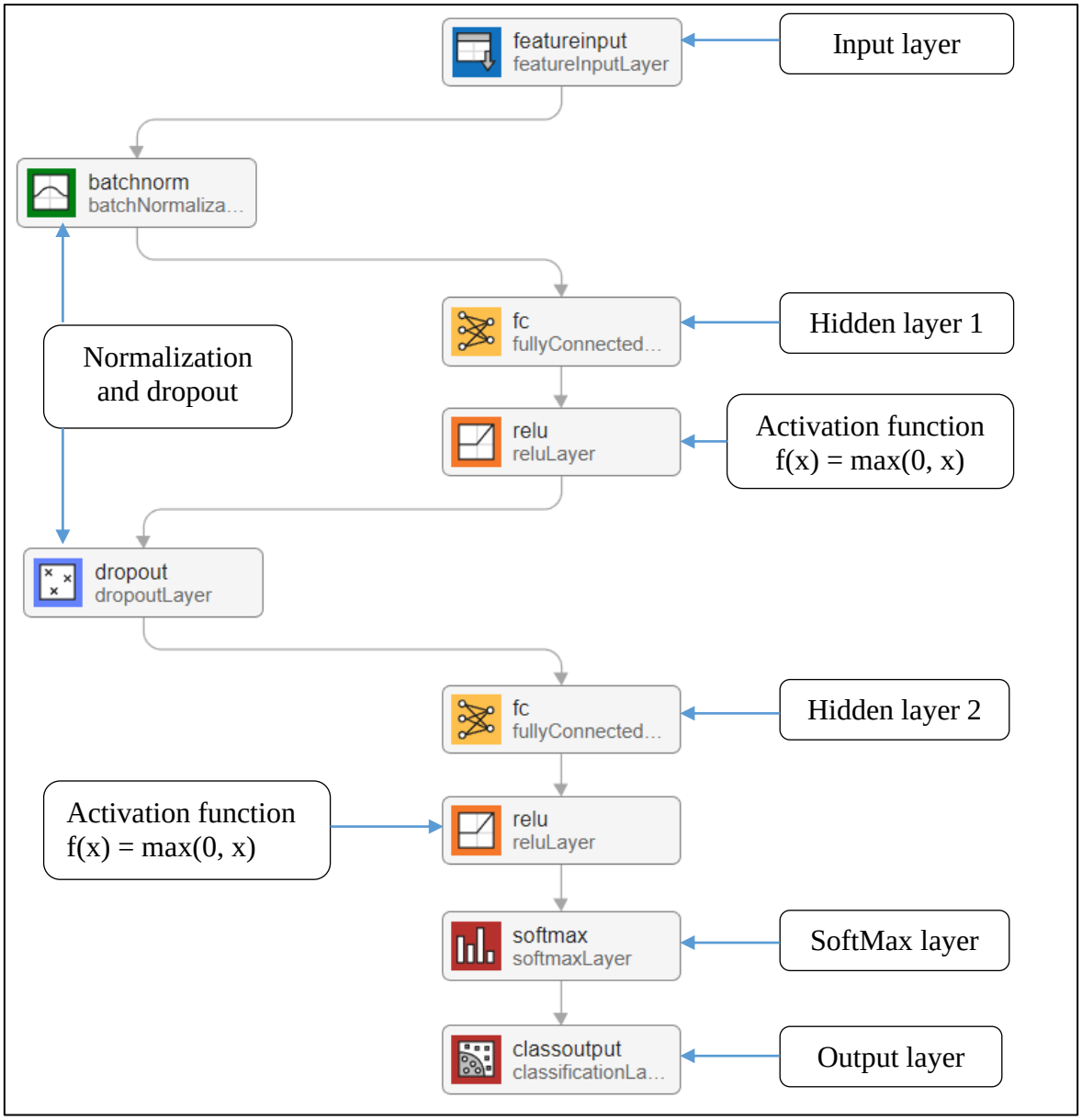

Figure 10. Architecture of fully connected neural network with input layer, 2 hidden layers, and classification output layer.

ReLU is a nonlinear activation function that mitigates the vanishing gradient problem and introduces beneficial non-linearity into the model. The ReLU function (f(x) = max(0, x)) is applied elementwise to the output of each neuron in these layers, introducing non-linearity and allowing the network to learn more complex patterns. To prevent overfitting, a dropout layer is included after the first layer as a regularization technique to prevent overfitting by randomly

setting a fraction of the input units to zero during training. In the multi-class classification, the output layer (class output) uses a SoftMax activation to convert the raw output scores from the layer into a probability distribution across classes. The architecture enables the network to process input data through multiple layers of abstraction, gradually transforming raw input into a form suitable for classification while maintaining good performance and generalization capabilities.

A hyperparameter search was performed to select the best number of neurons in each layer, learning rate, and batch size to achieve optimal performance. A repeated stratified 10-fold cross-validation technique was used to ensure that all training samples contributed to model training and validation. Finally, the test datasets were used to evaluate the performance of the trained model. The evaluation metrics included the overall accuracy, as well as accuracy values for individual classes predictions, The metrics were computed using a multiclass confusion matrix package from Python's Scikit-learn libraries. Furthermore, metrics such as the f1-score, precision, and recall were computed and presented in a tabular format.

4. RESULTS AND DISCUSSIONS

4.1. Hyperspectral image preprocessing results

The results from preprocessing the data with SG filter and SNV normalization technique are presented in Figure 11. These preprocessing techniques were selected due to their superior ability to discriminate between sugarbeet and kochia species. Furthermore, these methods have demonstrated an enhancement in classification accuracies for machine learning models (Shirzadifar et al., 2018). Figures 11a and 11b display the raw and preprocessed spectral signatures, respectively, while Figures 11c and 11d present the mean of the raw and preprocessed spectra for both sugarbeet and kochia species. These spectral signatures indicate the presence of chlorophyll absorption in the range of 500 to 590 nm.

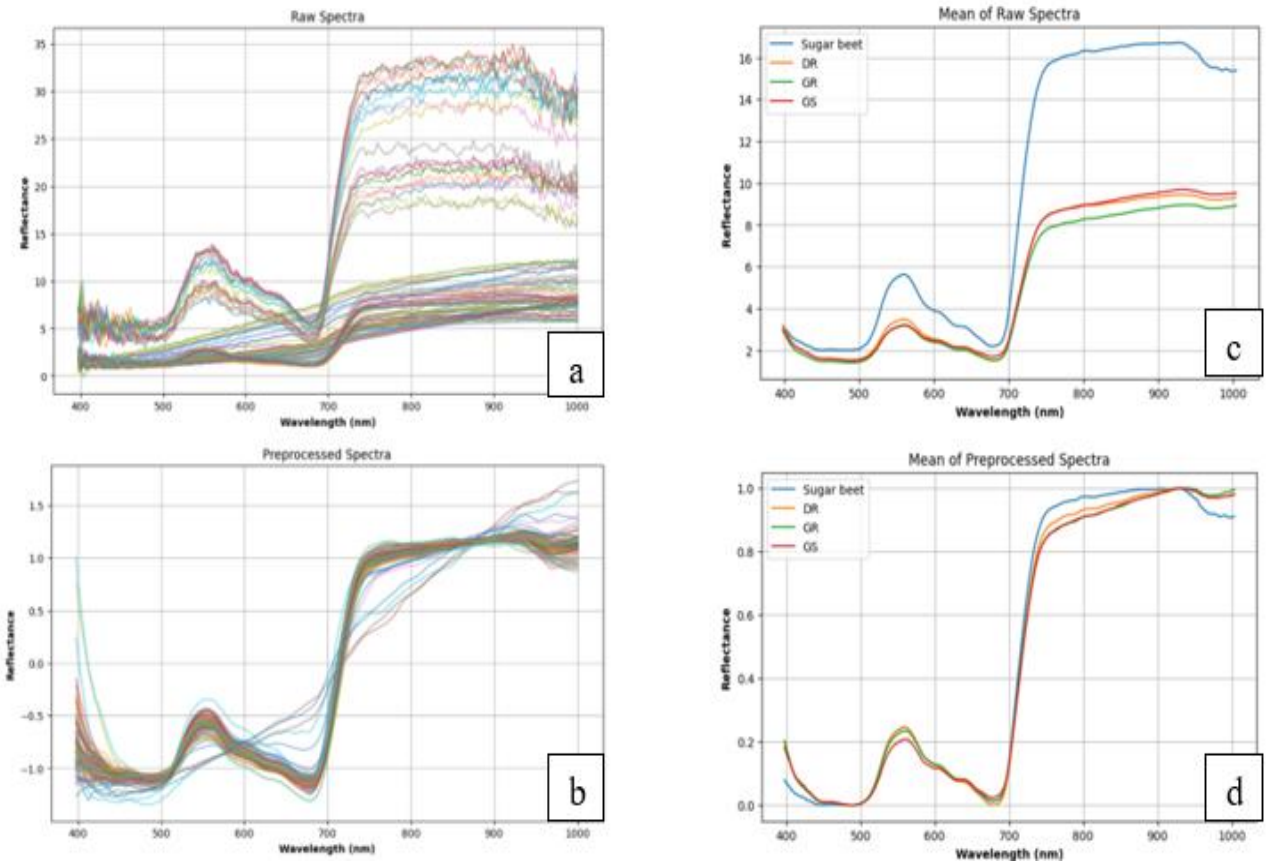

Figure 11. Hyperspectral data preprocessing using Savitzky-Golay filter and standard normal variate (SNV) to remove noise from the data.

A peak, associated with red edge reflection, is noticeable in Figure 8d, starting from 695 to 715 nm. The wavelengths spanning from 700 nm to 1000 nm correspond to the third overtone region, representing an excited state of molecules from their ground state (Graham Ram et al., 2023). These regions were selected using a feature selection algorithm to identify important wavelength features for machine learning. The mean spectral reflectance of kochia weed biotypes (DR, GR, and GS) and sugarbeet crop were analyzed to identify the most informative wavelength bands for classification. A recursive feature elimination was performed on the preprocessed hyperspectral reflectance data to select the most sensitive wavelength bands to classify the sugarbeet crop from 3 kochia biotypes. The wavelength bands ranging from 500 to 680 nm and 700 to 900 nm for greenhouse data, and 500 to 700 nm and 710 to 980 nm for field data, were identified as important spectrum regions for sugarbeet and kochia classification. These regions show distinct reflectance differences between sugarbeet, DR, GR, and GS kochia.

Additionally, spectral region between 500 and 800 nm has proven to be a crucial wavelength region for vegetation discrimination, consistently associated with chlorophyll content (Li et al., 2021). The observations of light reflectance variations across these spectral range not only enhance our understanding of specific biotypes but also underscore the potential of spectral data in differentiating between these kochia biotypes and sugarbeet.

4.1.1. Wavelength features selected using recursive feature elimination method

The feature selection technique was also employed as a dimensionality reduction algorithm, reducing the wavelength bands from 224 bands to 10 bands. The RFE-RF technique employed selected the important wavelength features for machine learning, providing a solution to the high dimensionality of hyperspectral data. The technique identified the relevant

wavelength bands with crucial spectral features to distinguish sugarbeet crops from kochia weeds (Table 5).

Table 5. Selected wavelength bands obtained using recursive feature elimination method.

Data	Wavelength Bands (nm)									
G^g	518.9	647.5	677.36	693.6	696.3	723.6	808.6	827.9	830.6	833.4
F^f	505.6	558.9	566.9	617.9	715.4	723.6	726.3	964.4	967.2	970

Note: G^g = Greenhouse data, F^f = Field data.

The results of wavelength bands selection using RFE-RF technique have similar weed identification characteristics to those found in studies by Li et al., (2021) and Huang et al., (2018). Respectively, the wavelength regions from 500 to 750 nm and 400 to 900 nm were identified as the most informative wavelength regions for differentiating between weed species. The study by Li et al., (2021) used hyperspectral images of *Carduus tenuiflorus Curtis (*thistle), *Setaria pumila* (yellow bristle grass), *Ranunculus acris* (buttercup), and *Anemanthele lessoniana* (wind grass) and employed principal component analysis (PCA) to select the most significant wavelength bands. Their study trained a Multilayer Perceptron (MLP) on these selected wavelength bands and achieved a prediction accuracy of 89.1%. Huang et al., (2018) used Fisher's Linear Discriminant Analysis (FLDA) to reduce dimensionality and selected 15 NIR wavelength bands to classify glyphosate-resistant and susceptible Italian ryegrass with a prediction accuracy between 75% and 80% using a maximum likelihood classifier. These findings, along with those from this research, support the claim that the near-infrared region has significant characteristics for distinguishing between crops and weeds.

The RFE-RF wavebands selection technique utilized in our study is supported by Ram et al., (2023), who also employed the RFE technique with a support vector machine (SVM) as the feature ranking criteria. They selected 10 significant wavelength bands for classifying palmer amaranth in a soybean field and achieved the highest prediction accuracy of 93.95% using a

quadratic discriminant analysis classifier. The higher accuracy demonstrates the flexibility and potential of the RFE technique, and its user-friendliness compared to PCA and FLDA for dimensionality reduction and wavelength bands selection. This emphasizes the effectiveness of the RFE technique in selecting informative wavelength bands for weed species classification. It offers clear advantages over traditional methods such as PCA and FLDA, such as the reduction in dimensionality and the identification of significant wavelength bands. The results achieved in this research and the parallel success of similar approaches in the literature demonstrated the potential of weed identification using waveband features within the spectrum range of 400-900 nm.

4.2. Classification results for sugarbeet and kochia biotypes

The deep neural network was used to predict the test samples after training and hyperparameter tuning. The prediction results from greenhouse and field experiments are shown in Table 6 and Table 7. The neural network achieved an overall prediction accuracy of 93.27% in the greenhouse experiment, with an F1-score of 0.93 (Table 6). The Cohen's kappa statistic, which measures the level of agreement between the model's predictions and the actual classifications, revealed a significant value of 0.93, with precision of 0.93.

Table 6. Summary of classification results on greenhouse data using the selected wavelength features.

Class	Classification (%)	Precision	Recall	F1-score
SB	97.5	0.99	0.97	0.98
DR	91.36	0.92	0.91	0.92
GR	87.5	0.88	0.88	0.88
GS	96.7	0.94	0.97	0.95
Overall Accuracy	93.27	0.93	0.93	0.93

Note: SB-sugarbeet, DR-dicamba-resistance, GR-glyphosate-resistant, and GS-glyphosate-susceptible.

The results from multiclass confusion matrices reveal that sugarbeet (SB), dicamba-resistant (DR), glyphosate-resistant (GR), and glyphosate-susceptible (GS) kochia were correctly identified with a prediction accuracy of 97.5 %, 91.36 %, 87.5 %, and 96.7 %, respectively (Figure 12a). This percentage indicates the fraction of spectra that were predicted correctly, specifically, the correct predictions for each class occur along the diagonal (upper-left to bottom-right), and incorrect predictions exist on either side of the diagonal. The neural network was subsequently trained on the spectral data acquired in the field.

Table 7 presents the classification results of GR kochia and sugarbeet. The model achieved a prediction accuracy of 98.76 %, indicating that about 99 out of every 100 spectra were correctly identified. For the field data, the trained model classified GR kochia and sugarbeet with a prediction accuracy of 98.56% and 98.96%, respectively.

Table 7. Summary of classification results on field data using the selected wavelength features.

Class	Classification (%)
SB	98.96
GR	98.56
Overall Accuracy	98.76

Note: SB-sugarbeet, GR-glyphosate-resistant.

The F1-score was 0.99, indicating a solid proportion of accurately predicted positive outcomes against the true positive spectra, with a precision of 0.99. The kappa score of 0.99 indicates how well the neural network's predictions match up with actual classifications (Figure 12b). The prediction results indicate a significant improvement in accuracy in distinguishing DR, GR, and GS compared to a study by Nugent et al., (2018) with a reported accuracy of 67%, 76%, and 80% for the same classification using support vector machine (SVM).

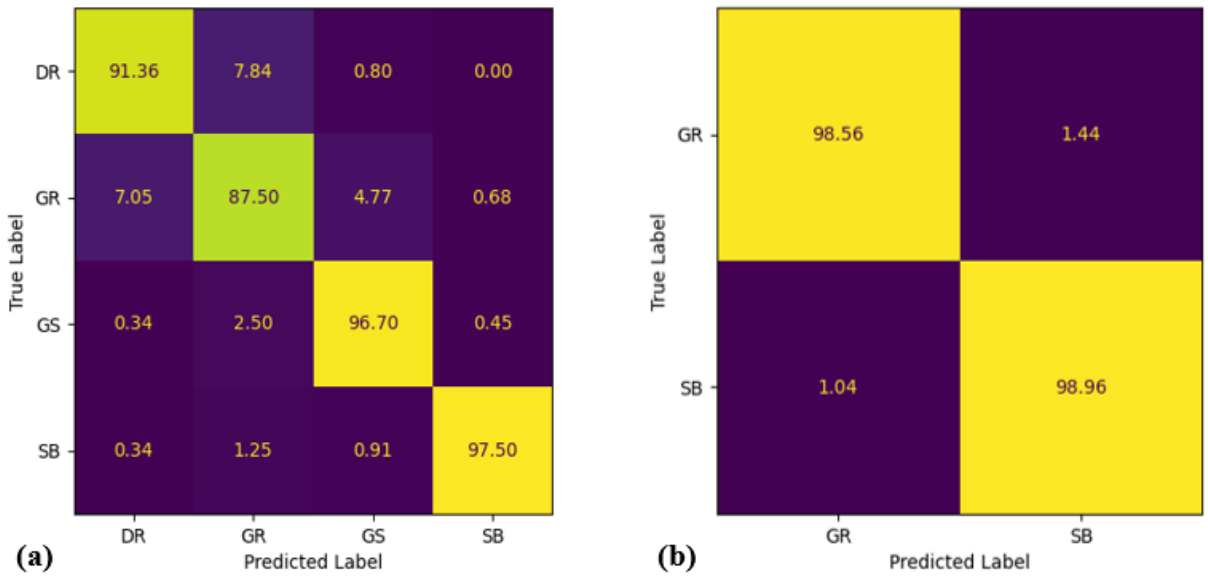

Figure 12. Multiclass confusion matrix (%) for sugarbeet (SB), dicamba-resistant (DR), glyphosate-resistant (GR) and glyphosate-susceptible (GS) kochia (a) greenhouse data (b) field data.

The accuracy in our study suggests the effectiveness and robustness of the neural network algorithm in accurately classifying kochia based on spectral data. Additionally, the study discovered that the classification accuracy showed correlation with the number of spectral samples used for model training. The neural network achieved optimal results when trained with a larger dataset, which enhanced the model's ability to generalize and accurately predict unseen datasets. It is important to note that the methods and order of preprocessing techniques applied to hyperspectral data significantly influenced the accuracy of the model's predictions. In this study, preprocessing the spectral data with SNV and SG smoothing significantly improved the model's ability to generalize from training to testing data. Preprocessing techniques applied to data in this research are identical to the steps by Graham Ram et al., (2023). Applying preprocessing technique like SNV is noted for increasing the prediction in a study by (Shirzadifar et al., 2018).

4.2.1. Prediction image using the trained machine learning model on testing images of sugarbeet and kochia biotypes

Hyperspectral images were randomly selected and preprocessed to remove the background. Subsequently, the 3D images were unfolded into a 2D array for prediction using the trained model. The trained model used the ten most important wavelengths selected by the Recursive Feature Elimination with Random Forest (RFE-RF) algorithm to predict the classes of the new images. The predicted 2D array was then folded back into 3D hyperspectral images using a logic mask developed during the image segmentation process. The prediction images were generated based on the predicted classes of the trained model. Figure 13 and Figure 14 illustrate the predictions on preprocessed testing hyperspectral images from the greenhouse and field experiment, respectively. In Figure 13, which shows the greenhouse predicted image using the trained model, it can be observed that some spectral pixels of DR kochia were misclassified as either GR or GS kochia.

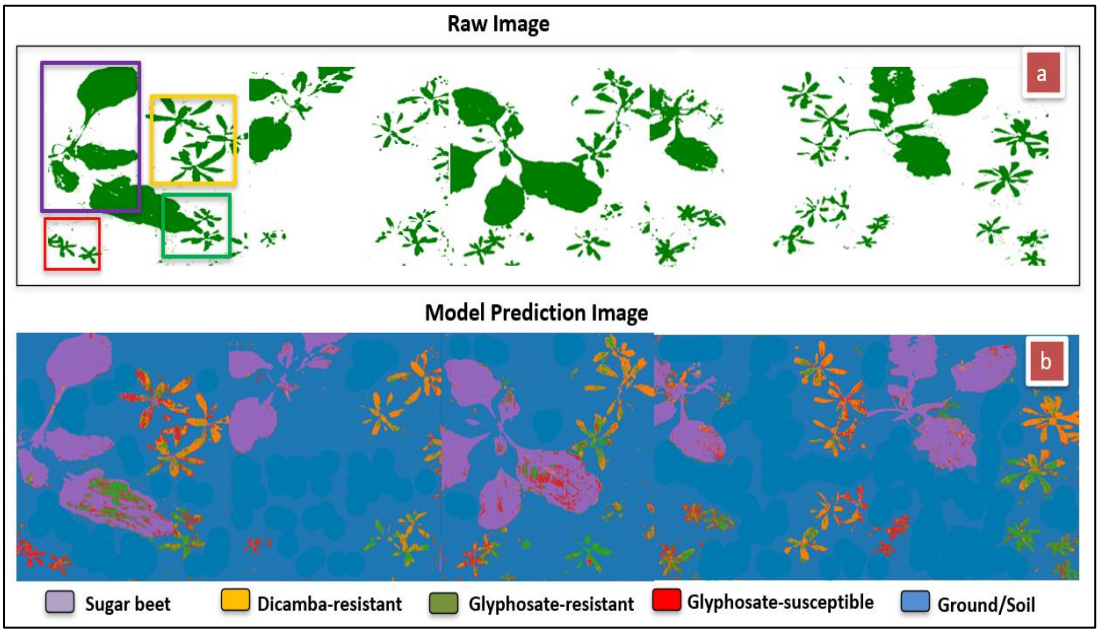

Figure 13. Prediction image generated by the trained model on greenhouse images, (a) raw image and (b) predicted image with color code indicating the spectra pixels that were classified as kochia or sugarbeet.

Additionally, there were instances where GR and GS kochia pixels were incorrectly classified as sugarbeet. This highlights the challenge in accurately distinguishing between the different classes in a multiclass classification task, where the model was trained to differentiate between sugarbeet, DR kochia, GR kochia, and GS kochia.

Likewise, Figure 14 presents the prediction results on field images to classify between sugarbeet and GR kochia. The results indicate that spectra pixels for sugarbeet were correctly classified by the model, demonstrating a high level of accuracy. However, it is noteworthy that a few pixels corresponding to background soil and dead plants leaves were misclassified as GR kochia.

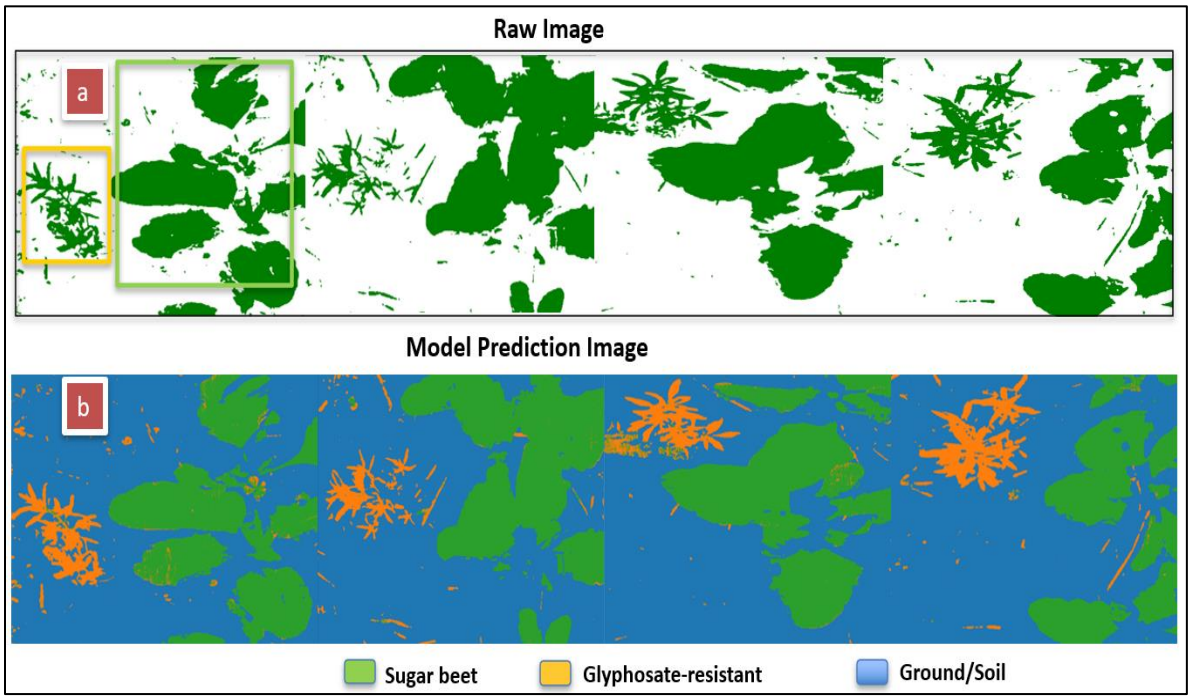

Figure14. Prediction image generated by the model on field images. (a) raw image (b) predicted image.

The distinction in the classification challenges between the greenhouse and field experiments is important to note. The greenhouse experiment required the model to perform multiclass classification, whereas the field experiment involved a simpler binary classification.

The predicted images highlight the potential of combining hyperspectral imaging with machine learning to effectively distinguish between resistant and susceptible kochia in sugarbeet, using distinct spectral signatures. Although there are some misclassifications between sugarbeet and kochia biotype pixels, the model's ability to accurately classify most pixels in both experimental settings demonstrate the potential and effectiveness in precision agricultural applications. This technology can be used to generate a prescription map to assist farmers in adopting herbicides for targeted weed management.

4.3. Assessment of herbicides on the reflectance of sugarbeet and kochia weed biotypes

The reflectance responses for DR, GR, and GS are illustrated Figure 15b, 15c, and 15d, respectively. The analysis of post-herbicide treatments provides a significant insight into the spectral reflectance patterns of sugarbeet, DR, GR, and GS kochia biotypes. The recorded variations in reflectance responses among individual kochia biotypes, particularly after treatment with acifluorfen and trisulfuron-methyl, underscore the differential susceptibility of these biotypes to herbicides. The lower reflectivity exhibited by DR kochia post acifluorfen treatment, a pattern also noted between GR and GS kochia, suggests potential differences in the physiological responses of these biotypes to this specific herbicide. Similarly, the distinct reflectance patterns in the near-infrared region (750-1000 nm) following trisulfuron-methyl treatment indicate differential herbicide uptake or metabolic responses among the biotypes. The results presented in Figure 15b reveal significant differences in the reflectance patterns of DR following various treatments. Specifically, all treated DR kochia exhibited significantly lower reflectance compared to the untreated group. This suggests that the applied treatments may have induced physiological changes in the DR kochia, leading to decreased reflectance. In contrast, the reflectance patterns for GR and GS kochia showed a different trend.

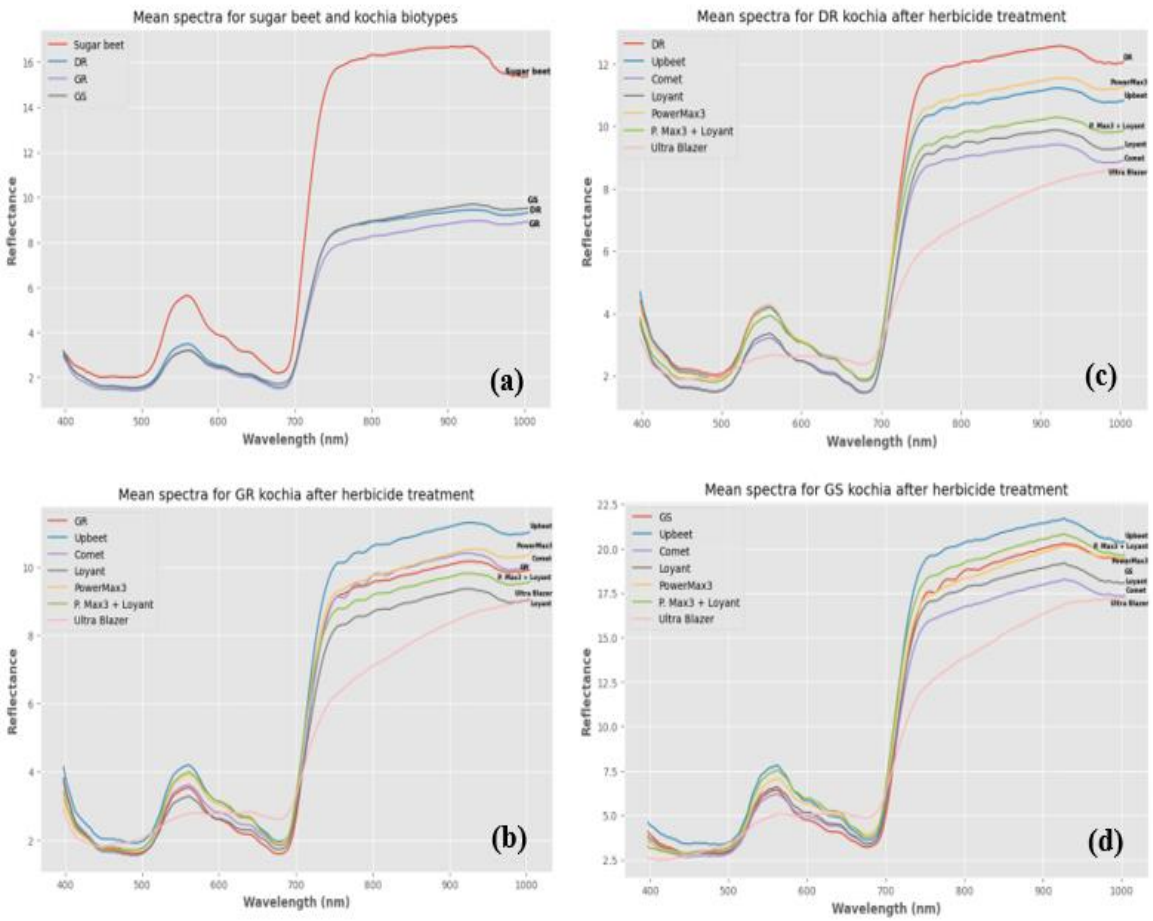

Figure 15. Mean reflectance spectra for sugarbeet and kochia biotypes after herbicide treatment in the greenhouse experiment a) DR, GR, and GS kochia b) GR after treatment c) DR after treatment d) GS after treatment.

For GR kochia, treatments with trisulfuron-methyl, fluroxypyr-ester, and glyphosate resulted in higher reflectance than the untreated GR group (Figure 15c). Similarly, for GS kochia, treatments with trisulfuron-methyl and glyphosate + florpyrauxifen-benzyl led to significantly higher reflectance than the untreated GS group (Figure 15d). These observations indicate that these treatments may have caused different physiological responses in the GR and GS kochia biotypes, resulting in increased reflectance.

These findings highlight the potential utilization of the spectral reflectance properties in assessing herbicide efficacy and the susceptibility of specific kochia biotypes to herbicide

applications. By leveraging these reflectance characteristics, more targeted and effective herbicide management strategies can be developed. This could aid in the creation of prescription maps for precise herbicide application, potentially improving weed control outcomes while minimizing herbicide use and associated environmental impacts. However, further research is needed to fully understand the underlying mechanisms driving these observed spectral reflectance variations post-herbicide treatment. Additionally, the practical implementation of these findings in real-world agricultural settings would require the development of suitable spectral imaging technologies and data interpretation algorithms. Nonetheless, this study represents a promising step towards more sustainable and effective weed management strategies.

The study further assessed the effectiveness of six different herbicides to control and kill DR, GR, and GS kochia weed biotypes in a sugarbeet field. The results of this study provide valuable insights into the effectiveness of different herbicides in controlling and managing DR, GR, and GS kochia weed biotypes in a sugarbeet field. It was observed that all three kochia biotypes showed resistance to trisulfuron-methyl, fluroxypyr-ester, and florpyrauxifen-benzyl, which indicates that these treatments were less ineffective to control or kill the kochia (Figure 16b, 16c, 16d, and Fig 17b, 17d, 17c). This suggests that while these treatments can control broad-leaf weeds in sugarbeet crops, they are ineffective in controlling the kochia biotypes and could potentially lead to the emergence of more resistant biotypes.

This suggests that while these treatments can control broad-leaf weeds in sugarbeet crops, they are ineffective in controlling the kochia biotypes and could potentially lead to the emergence of more resistant biotypes. Interestingly, the application of fluroxypyr-ester and acifluorfen had a negative impact on the sugarbeet, causing leaf shrinkage, stunted growth (Figure 16c & 17c), significant leaf burns, and bronzing (Figure 16g & 17g).

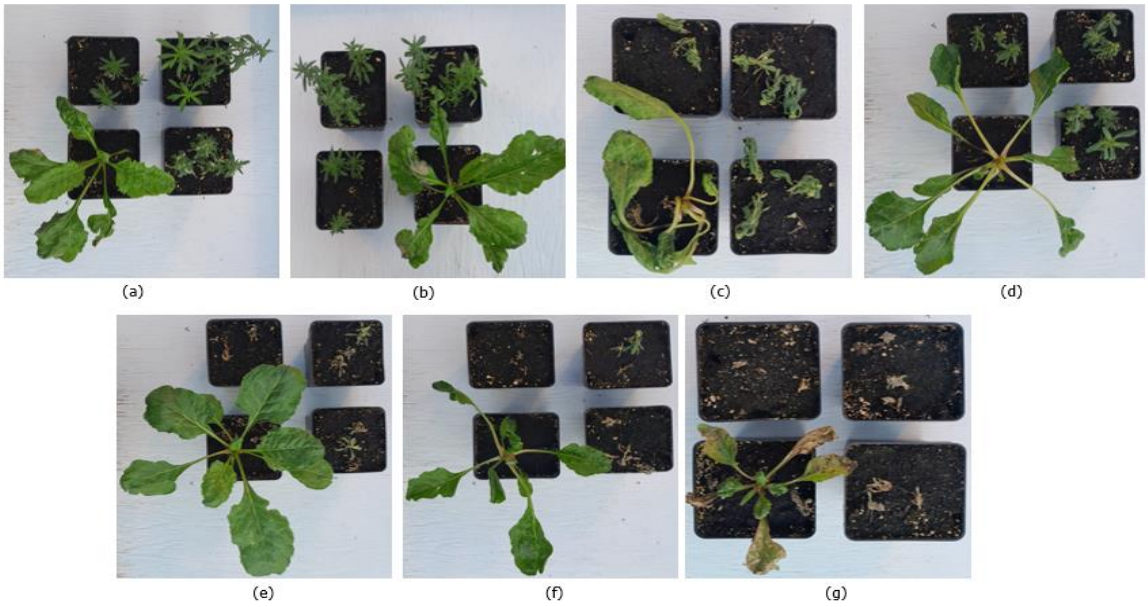

Figure 16. Treatments effects on kochia and sugarbeet during greenhouse experiment a) Untreated group b) trisulfuron-methyl c) fluroxypyr-ester d) florpyrauxifen-benzyl e) glyphosate f) glyphosate + florpyrauxifen-benzyl g) acifluorfen.

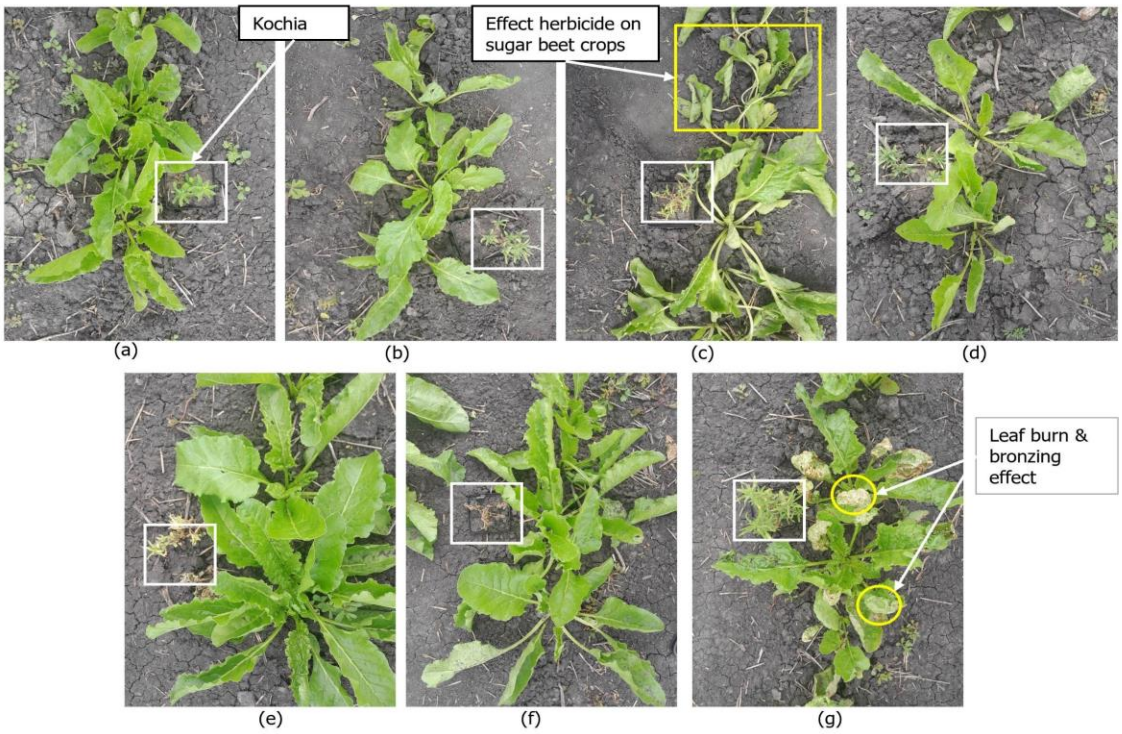

Figure 17. Herbicide treatments on kochia and sugarbeet and their effect a) Untreated plants b) trisulfuron-methyl c) fluroxypyr-ester d) florpyrauxifen-benzyl e) glyphosate f) glyphosate + florpyrauxifen-benzyl g) acifluorfen.

The negative impact of fluroxypyr-ester and acifluorfen on sugarbeet crops highlights the importance of selectivity in herbicide application. Conversely, treatments with glyphosate and a combination of glyphosate and florpyrauxifen-benzyl were found to be effective in controlling all kochia biotypes, without causing any physical harm or damage to the sugarbeet (Fig 16e, 16f, 17e, and 17f). The results highlight the potential of a synergistic combination of glyphosate and florpyrauxifen-benzyl in quickly and effectively controlling DR, GR, and GS kochia weeds. This strategy of combining more than two herbicides with more than one mode of action could potentially address the ongoing issue of herbicide-resistant weeds and underscores the importance of integrated weed management in controlling herbicide-resistant weed (Kumar & Jha, 2015). However, the implementation of this strategy requires careful planning and management, such as the timing of herbicide application, the specific weeds present in the field. The findings of the herbicide treatment experiment demonstrate that strategic planning and integrated herbicide application strategies are vital for successful weed management, ensuring sustainable crop production while minimizing the risk of herbicide resistance. However, further research is needed to validate these findings in different environmental conditions and to explore other potential strategies for effective weed management.

4.3.1. Limitations of the research

There were some limitations and challenges during planting, data collection and imaging processing. In both greenhouse and field experiments, the number of scanned kochia and sugarbeet plants was constrained due to weather conditions and the shorter growing season for sugarbeet planting. Additionally, the field experiment was restricted to using only glyphosate-resistant kochia, as dicamba-resistant and glyphosate-susceptible kochia had poor germination rates. This limitation precluded comparative analysis and contributed to variations in overall

classification of the trained model. Moreover, the data collection platform was semi-automated, necessitating manual movement to each data collection point, which further limited the number of images captured. Automating this process could potentially increase images captured, thereby increasing the datasets for training classification in future studies. To mitigate these challenges, extending the study period and automating data collection are recommended strategies to improve the number of images captured for machine learning.

5. CONCLUSIONS

Early weed detection of herbicide-resistant and susceptible kochia has been a challenging task due to the similarities of leaves shape and size. Kochia's efficient seed production and spread make it adaptable to herbicides, leading to herbicide-resistant populations, posing a significant challenge for effective weed control strategies. The field and greenhouse experiments demonstrate the potential of hyperspectral imaging technology and a deep neural network to differentiate herbicide-resistant and susceptible kochia in sugarbeet. Although herbicide-resistant and susceptible kochia have similar physiological features during early growth stage but this research showed that dicamba-resistant, glyphosate-resistant, and glyphosate-susceptible kochia weeds have distinguishable spectral reflectance characteristics from sugarbeet crops.

The experiments revealed that sugarbeet reflects more light in the visible and infrared regions of the electromagnetic spectrum compared to kochia weed. The experiments identified the spectrum region from 500-680 nm and 700-980 nm as the wavelength bands containing the most relevant spectral information for discriminating between kochia biotypes and sugarbeet. The identified wavelength features in this research used to distinguish between herbicide-resistant and susceptible kochia in sugarbeet are supported by literature. This indicates that spectral features in the 400-1000 nm wavelength region are particularly significant for weed and crop identification.

The fully connected neural network classified sugarbeet and kochia biotypes based on spectral reflectance characteristics, achieving a prediction accuracy of 93.27% in greenhouse experiment and 98.76% for field data. It was observed that the features selected wavelength bands significantly influenced the prediction accuracy of the model. That is selecting the important wavelength features to train a model will result in higher prediction accuracy. This

highlights the need for future studies to identify significant wavelength bands for model training, especially for weed detection. The study further showed that RFE-RF is an effective method for reducing the high dimensionality of hyperspectral data and more importantly a technique for selecting important spectral features for classification.

The herbicide assessment indicates that combining more than one herbicide mode of action presents an effective strategy to control resistant kochia weeds in sugarbeet. This highlights the importance of implementing integrated herbicide weed management strategies to mitigate the emergence of herbicide-resistant species. The findings can assist weed control in sugarbeet by applying herbicides based on the unique spectral reflectance of identified kochia and this approach will prevent the emergence of resistant kochia biotypes.

Future research should focus on developing automated data acquisition and image processing technologies to identify and manage kochia in sugarbeet. By leveraging the unique spectral signature, these advancements can enhance the identification and control of herbicide-resistant kochia in sugarbeet.

REFERENCES

Arias, F., Zambrano, M., Broce, K., Medina, C., Pacheco, H., & Nunez, Y. (2020). Hyperspectral imaging for rice cultivation: Applications, methods and challenges. *AIMS Agriculture and Food*, *6*(1), 273–307. https://doi.org/10.3934/AGRFOOD.2021018

Aslan, M. F., Durdu, A., Sabanci, K., Ropelewska, E., & Gültekin, S. S. (2022). A Comprehensive Survey of the Recent Studies with UAV for Precision Agriculture in Open Fields and Greenhouses. *Applied Sciences (Switzerland)*, *12*(3). https://doi.org/10.3390/app12031047

Babu, A. S., & Adeyeye, S. A. O. (2023). Extraction of sugar from sugar beets and cane sugar. *In Extraction Processes in the Food Industry* (177–196). https://doi.org/10.1016/B978-0-12-819516-1.00007-7

Beckie, H. J., Blackshaw, R. E., Leeson, J. Y., Stahlman, P. W., Gaines, T. A., & Johnson, E. N. (2018). Seedbank persistence, germination and early growth of glyphosate-resistant Kochia scoparia. *Weed Research*, *58*(3), 177–187. https://doi.org/10.1111/wre.12294

Burger, J., & Geladi, P. (2005). Hyperspectral NIR image regression part I: Calibration and correction. *Journal of Chemometrics*, *19*(5–7), 355–363. https://doi.org/10.1002/cem.938

Burger, J., & Geladi, P. (2006). Hyperspectral NIR image regression part II: Dataset preprocessing diagnostics. *Journal of Chemometrics*, *20*(3–4), 106–119. https://doi.org/10.1002/cem.986

Chang, C. Y., Zhou, R., Kira, O., Marri, S., Skovira, J., Gu, L., & Sun, Y. (2020). An Unmanned Aerial System (UAS) for concurrent measurements of solar-induced chlorophyll fluorescence and hyperspectral reflectance toward improving crop monitoring. Agricultural and Forest Meteorology, 294. https://doi.org/10.1016/j.agrformet.2020.108145.

De Juan, A., Piqueras, S., Maeder, M., Hancewicz, T., Duponchel, L., & Tauler, R. (2014). *2 Chemometric Tools for Image Analysis*. https://doi.org/10.1002/9783527678136.ch2

Diao, Z., Guo, P., Zhang, B., Yan, J., He, Z., Zhao, S., Zhao, C., & Zhang, J. (2023). Spatial-spectral attention-enhanced Res-3D-OctConv for corn and weed identification utilizing hyperspectral imaging and deep learning. *Computers and Electronics in Agriculture*, *212*. https://doi.org/10.1016/j.compag.2023.108092

Esposito, M., Crimaldi, M., Cirillo, V., Sarghini, F., & Maggio, A. (2021). Drone and sensor technology for sustainable weed management: a review. *Chemical and Biological Technologies in Agriculture*, *8*(1), 18. https://doi.org/10.1186/s40538-021-00217-8

Geddes, C. M., & Sharpe, S. M. (2022). Crop yield losses due to kochia (Bassia scoparia) interference. *Crop Protection*, *157*(March), 105981. https://doi.org/10.1016/j.cropro.2022.105981

Graham Ram, B., Zhang, Y., Costa, C., Raju Ahmed, M., Peters, T., Jhala, A., Howatt, K., & Sun, X. (2023). Palmer amaranth identification using hyperspectral imaging and machine learning technologies in soybean field. *Computers and Electronics in Agriculture*, *215*, 108444. https://doi.org/10.1016/j.compag.2023.108444

Heap, I., & Duke, S. O. (2018). Overview of glyphosate-resistant weeds worldwide. *Pest Management Science*, *74*(5), 1040–1049. https://doi.org/10.1002/ps.4760

Heap, I. The International Herbicide-Resistant Weed Database. (May 21, 2024) . Available www.weedscience.org.

Huang, Y., Lee, M. A., Nandula, V. K., & Reddy, K. N. (2018). Hyperspectral Imaging for Differentiating Glyphosate-Resistant and Glyphosate-Susceptible Italian Ryegrass. *American Journal of Plant Sciences*, *09*(07), 1467–1477. https://doi.org/10.4236/ajps.2018.97107

Istiak, Md. A., Syeed, M. M. M., Hossain, M. S., Uddin, M. F., Hasan, M., Khan, R. H., & Azad, N. S. (2023). Adoption of Unmanned Aerial Vehicle (UAV) imagery in agricultural management: A systematic literature review. Ecological Informatics, 78, 102305. https://doi.org/10.1016/j.ecoinf.2023.102305

Kanthi, M., Hitendra Sarma, T., & Shobha Bindu, C. (2020). A 3d-Deep CNN based feature extraction and hyperspectral image classification. *2020 IEEE India Geoscience and Remote Sensing Symposium, InGARSS 2020 - Proceedings*, 229–232. https://doi.org/10.1109/InGARSS48198.2020.9358920

Khan, A., Vibhute, A. D., Mali, S., & Patil, C. H. (2022). A systematic review on hyperspectral imaging technology with a machine and deep learning methodology for agricultural applications. In *Ecological Informatics* (Vol. 69). Elsevier B.V. https://doi.org/10.1016/j.ecoinf.2022.101678

Kumar, V., & Jha, P. (2015). Effective Preemergence and Postemergence Herbicide Programs for Kochia Control. *Weed Technology*, *29*(1), 24–34. https://doi.org/10.1614/WT-D-14-00026.1

Kumar, V., Jha, P., Jugulam, M., Yadav, R., & Stahlman, P. W. (2019). Herbicide-resistant kochia (Bassia scoparia) in North America: A review. *Weed Science*, *67*(1), 4–15. https://doi.org/10.1017/wsc.2018.72

Kumar, V., Jha, P., & Reichard, N. (2014). Occurrence and Characterization of Kochia (Kochia scoparia) Accessions with Resistance to Glyphosate in Montana . *Weed Technology*, *28*(1), 122–130. https://doi.org/10.1614/wt-d-13-00115.1

Kumar, V., Liu, R., Currie, R. S., Jha, P., Morran, S., Gaines, T., & Stahlman, P. W. (2021). Cross-resistance to atrazine and metribuzin in multiple herbicide-resistant kochia accessions: Confirmation, mechanism, and management. *Weed Technology*, *35*(4), 539–546. https://doi.org/10.1017/wet.2020.141

Lauwers, M., De Cauwer, B., Nuyttens, D., Cool, S. R., & Pieters, J. G. (2020). Hyperspectral Classification of Cyperus esculentus Clones and Morphologically Similar Weeds. *Sensors*, *20*(9), 2504. https://doi.org/10.3390/s20092504

Lauwers, M., Nuyttens, D., De Cauwer, B., & Pieters, J. (2022). Hyperspectral classification of poisonous solanaceous weeds in processing Phaseolus vulgaris L. and Spinacia oleracea L. *Computers and Electronics in Agriculture*, *196*, 106908. https://doi.org/10.1016/j.compag.2022.106908

Lee, M. A., Huang, Y., Nandula, V. K., & Reddy, K. N. (2014). Differentiating glyphosate-resistant and glyphosate-sensitive Italian ryegrass using hyperspectral imagery. *Sensing for Agriculture and Food Quality and Safety VI*, *9108*, 91080B. https://doi.org/10.1117/12.2053072

Li, Y., Al-Sarayreh, M., Irie, K., Hackell, D., Bourdot, G., Reis, M. M., & Ghamkhar, K. (2021). Identification of Weeds Based on Hyperspectral Imaging and Machine Learning. *Frontiers in Plant Science*, *11*. https://doi.org/10.3389/fpls.2020.611622

Li, Y. H., Tan, X., Zhang, W., Jiao, Q. Bin, Xu, Y. X., Li, H., Zou, Y. B., Yang, L., & Fang, Y. P. (2021). Research and Application of Several Key Techniques in Hyperspectral Image Preprocessing. *Frontiers in Plant Science*, *12*. https://doi.org/10.3389/fpls.2021.627865

Li, B., Fang, L., Chen, N., Kang, J., & Yue, J. (2024). Enhancing Hyperspectral Image Classification: Leveraging Unsupervised Information with Guided Group Contrastive Learning. *IEEE Transactions on Geoscience and Remote Sensing*, *62*, 1–17. https://doi.org/10.1109/TGRS.2024.3350700

Liu, J., Feng, Y., Liu, W., Orlando, D., & Li, H. (2020). Training data assisted anomaly detection of multi-pixel targets in hyperspectral imagery. *IEEE Transactions on Signal Processing*, *68*, 3022–3032. https://doi.org/10.1109/TSP.2020.2991311

López-Granados, F. (2011). Weed detection for site-specific weed management: Mapping and real-time approaches. *Weed Research*, *51*(1), 1–11. https://doi.org/10.1111/j.1365-3180.2010.00829.x

Mishra, P., Lohumi, S., Ahmad Khan, H., & Nordon, A. (2020). Close-range hyperspectral imaging of whole plants for digital phenotyping: Recent applications and illumination correction approaches. In *Computers and Electronics in Agriculture* (Vol. 178). Elsevier B.V. https://doi.org/10.1016/j.compag.2020.105780

Mosqueda, E. G., Lim, C. A., Sbatella, G. M., Jha, P., Lawrence, N. C., & Kniss, A. R. (2020). Effect of crop canopy and herbicide application on kochia (Bassia scoparia) density and seed production. *Weed Science*, *68*(3), 278–284. https://doi.org/10.1017/wsc.2020.23

Nugent, P. W., Shaw, J. A., Jha, P., Scherrer, B., Donelick, A., & Kumar, V. (2018). Discrimination of herbicide-resistant kochia with hyperspectral imaging. *Journal of Applied Remote Sensing*, *12*(01), 1. https://doi.org/10.1117/1.jrs.12.016037

Paoletti, M. E., Haut, J. M., Plaza, J., & Plaza, A. (2019). Deep learning classifiers for hyperspectral imaging: A review. In *ISPRS Journal of Photogrammetry and Remote Sensing* (Vol. 158, pp. 279–317). Elsevier B.V. https://doi.org/10.1016/j.isprsjprs.2019.09.006

Piqueras, S., Duponchel, L., Tauler, R., & De Juan, A. (2011). Resolution and segmentation of hyperspectral biomedical images by Multivariate Curve Resolution-Alternating Least Squares. *Analytica Chimica Acta*, *705*(1–2), 182–192. https://doi.org/10.1016/j.aca.2011.05.020

Pott, L. P., Amado, T. J. C., Schwalbert, R. A., Sebem, E., Jugulam, M., & Ciampitti, I. A. (2020). Pre-planting weed detection based on ground field spectral data. *Pest Management Science*, *76*(3), 1173–1182. https://doi.org/10.1002/ps.5630

Rai, N., Zhang, Y., Ram, B. G., Schumacher, L., Yellavajjala, R. K., Bajwa, S., & Sun, X. (2023). Applications of deep learning in precision weed management: A review. *Computers and Electronics in Agriculture*, *206*. https://doi.org/10.1016/j.compag.2023.107698

Ram, B. G., Oduor, P., Igathinathane, C., Howatt, K., & Sun, X. (2024). A systematic review of hyperspectral imaging in precision agriculture: Analysis of its current state and prospects. *Computers and Electronics in Agriculture*, *222*, 109037. https://doi.org/10.1016/J.COMPAG.2024.109037

Savitzky, A., & Golay, M. J. E. (1951). Smoothing and Differentiation of Data by Simplified Least Squares Procedures. In *Z. Physiological Chemistry* (Vol. 40, Issue 2). https://pubs.acs.org/sharingguidelines

Sbatella, G. M., Adjesiwor, A. T., Kniss, A. R., Stahlman, P. W., Westra, P., Moechnig, M., & Wilson, R. G. (2019). Herbicide options for glyphosate-resistant kochia (Bassia scoparia) management in the Great Plains. *Weed Technology*, *33*(5), 658–663. https://doi.org/10.1017/wet.2019.48

Scherrer, B., Sheppard, J., Jha, P., & Shaw, J. A. (2019). Hyperspectral imaging and neural networks to classify herbicide-resistant weeds. *Journal of Applied Remote Sensing*, *13*(04), 1. https://doi.org/10.1117/1.jrs.13.044516

Shirzadifar, A., Bajwa, S., Mireei, S. A., Howatt, K., & Nowatzki, J. (2018). Weed species discrimination based on SIMCA analysis of plant canopy spectral data. *Biosystems Engineering*, *171*, 143–154. https://doi.org/10.1016/J.BIOSYSTEMSENG.2018.04.019

Shirzadifar, A., Bajwa, S., Nowatzki, J., & Shojaeiarani, J. (2020b). Development of spectral indices for identifying glyphosate-resistant weeds. *Computers and Electronics in Agriculture*, *170*. https://doi.org/10.1016/j.compag.2020.105276

Sunil, G., C., Zhang, Y., Koparan, C., Ahmed, M. R., Howatt, K., & Sun, X. (2022). Weed and crop species classification using computer vision and deep learning technologies in greenhouse conditions. *Journal of Agriculture and Food Research*, *9*(May), 100325. https://doi.org/10.1016/j.jafr.2022.100325

Torbiak, A. T., Blackshaw, R. E., Brandt, R. N., Hamman, B., & Geddes, C. M. (2021). Herbicide strategies for managing glyphosate-resistant and-susceptible kochia (Bassia scoparia) in spring wheat. *Canadian Journal of Plant Science*, *101*(4), 607–621. https://doi.org/10.1139/cjps-2020-0303

United States Department of Agriculture, National Agricultural Statistical Services, June 2022 Report. Available online at https://www.nass.usda.gov. Accessed on June 9, 2024.

Vélez, S., Martínez-Peña, R., & Castrillo, D. (2023). Beyond Vegetation: A Review Unveiling Additional Insights into Agriculture and Forestry through the Application of Vegetation Indices. *J*, *6*(3), 421–436. https://doi.org/10.3390/j6030028

Wang, A., Zhang, W., & Wei, X. (2019). A review on weed detection using ground-based machine vision and image processing techniques. In *Computers and Electronics in Agriculture* (Vol. 158, pp. 226–240). Elsevier B.V. https://doi.org/10.1016/j.compag.2019.02.005

Westra, E. P., Nissen, S. J., Getts, T. J., Westra, P., & Gaines, T. A. (2019). The survey reveals frequency of multiple resistance to glyphosate and dicamba in kochia (Bassia scoparia). *Weed Technology*, *33*(5), 664–672. https://doi.org/10.1017/wet.2019.54

Wieme, J., Mollazade, K., Malounas, I., Zude-Sasse, M., Zhao, M., Gowen, A., Argyropoulos, D., Fountas, S., & Van Beek, J. (2022). Application of hyperspectral imaging systems and artificial intelligence for quality assessment of fruit, vegetables and mushrooms: A review. In *Biosystems Engineering* (Vol. 222, pp. 156–176). Academic Press. https://doi.org/10.1016/j.biosystemseng.2022.07.013

Xu, B., Fan, J., Chao, J., Arsenijevic, N., Werle, R., & Zhang, Z. (2023). Instance segmentation method for weed detection using UAV imagery in soybean fields. *Computers and Electronics in Agriculture*, *211*. https://doi.org/10.1016/j.compag.2023.107994

Zhang, Y., Wang, M., Zhao, D., Liu, C., & Liu, Z. (2023). Early weed identification based on deep learning: A review. *Smart Agricultural Technology*, *3*. https://doi.org/10.1016/j.atech.2022.100123

APPENDIX A: SUGARBEET, KOCHIA, AND HERBICIDES UTILIZED FOR THE EXPERIMENT

Table A1. Sugarbeet kochia varieties for greenhouse and field experiments.

Experiment	Sugarbeet variety
Greenhouse	Sugarbeet hybrid (BTS 8927 Betaseed, KWS Seeds, Minneapolis, MN, 2022)
Field	Sugarbeet variety CR 793 (Crystal Sugarbeet, Moorhead, MN)

Table A2. Kochia biotypes and their resistant characteristics.

Kochia weed species	Trait
DR	Dicamba-resistant
GR	Glyphosate-resistant
GS	Glyphosate-susceptible

Note: DR-dicamba-resistant, GR-glyphosate-resistant, and GS-glyphosate-susceptible kochia

Table A3. Herbicides applied to sugarbeet and kochia.

Common names	Trade name	Mode of action/group
Trisulfuron-methyl	Upbeet	ALS/ Group 2
Fluroxypyr-ester	Comet	Synthetic auxins/ Group 4
Florpyrauxifen-benzyl	Rinksor	Synthetic auxins/ Group 4
Glyphosate	Roundup PowerMax3	Inhibition of EPSP/ Group 9
Glyphosate + florpyrauxifen-benzyl	Roundup PowerMax3 + Rinksor	Synthetic auxins + Inhibition of EPSP
Acifluorfen	Ultra Blazer	PPO / Group 14

Note: ALS-Acetolactate synthase, ESPS-Inhibits 5-enopyruvylshikimae-3-phosphaste, and PPO-Protoporphyrinogen Oxidase.

APPENDIX B: PLANTING, DATA COLLECTION AND IMAGE PREPROCESSING OF KOCHIA AND SUGARBEET

Figure B1. Casselton agronomy seed research field utilized for planting sugarbeet and kochia.

Figure B2. Illustration of sugarbeet planted in rows on the field for effective data collection.

Figure B3. Planting kochia in greenhouse pots for greenhouse experiment.

Figure B4. Kochia and sugarbeet 3 weeks old prior to data collection in the greenhouse.

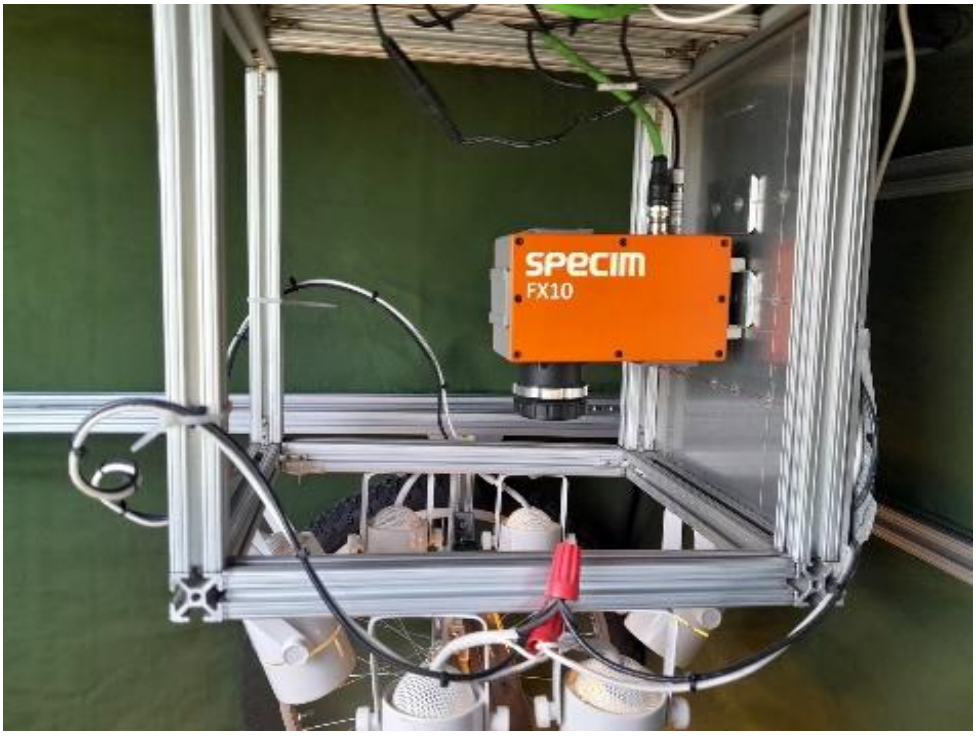

Figure B5. Hyperspectral sensor (Specim FX10) mounted on data collection platform utilized to record images in greenhouse and field.

Figure B6. Capturing white reference image and raw image with the sensor with tarp covering the platform to minimize external effects like wind and sunlight.

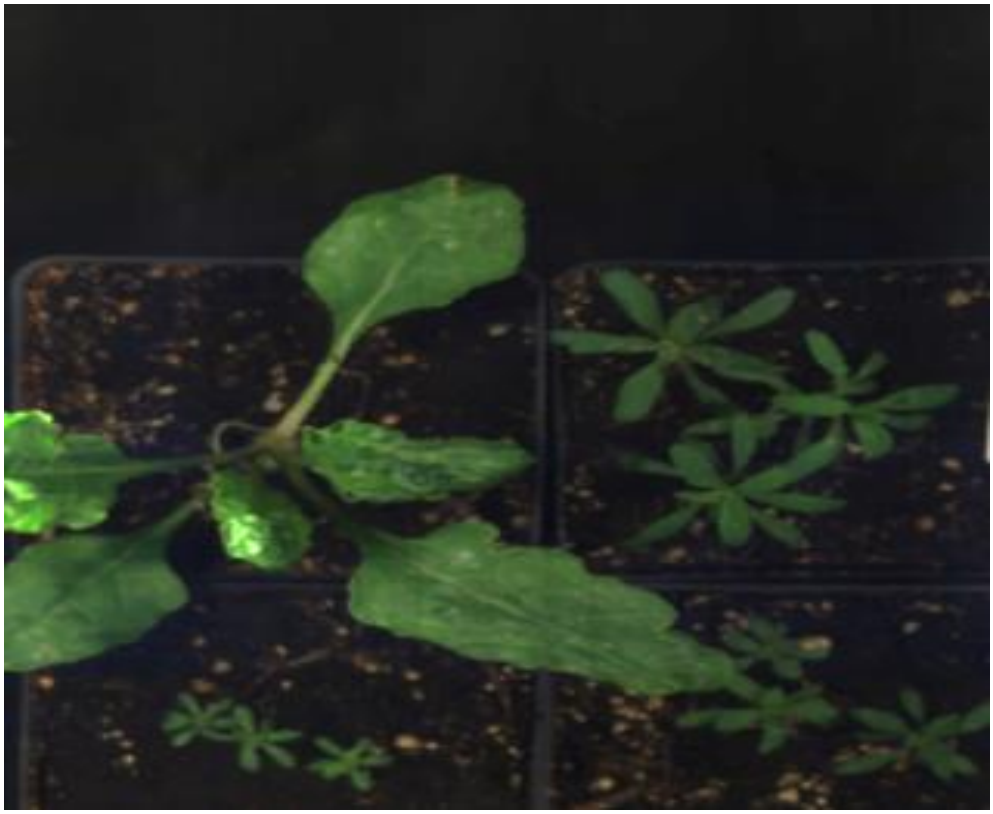

Figure B7. Calibrated RGB image using white and dark reference images.

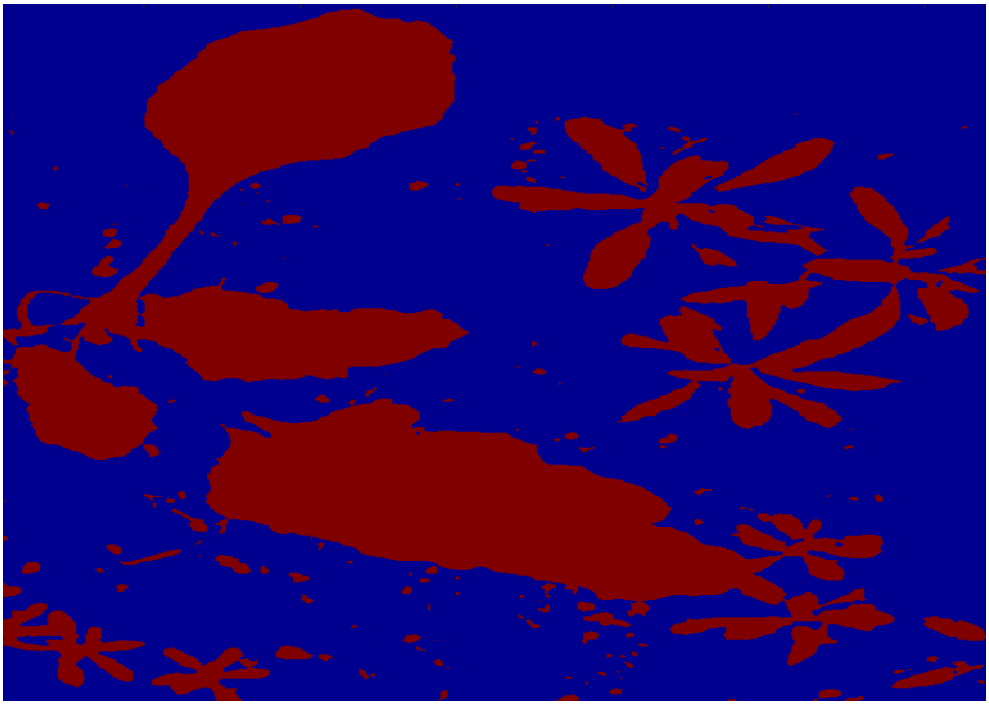

Figure B8. Application of k-means clustering algorithm (number of clusters = 2) to remove soil background from calibrated image.

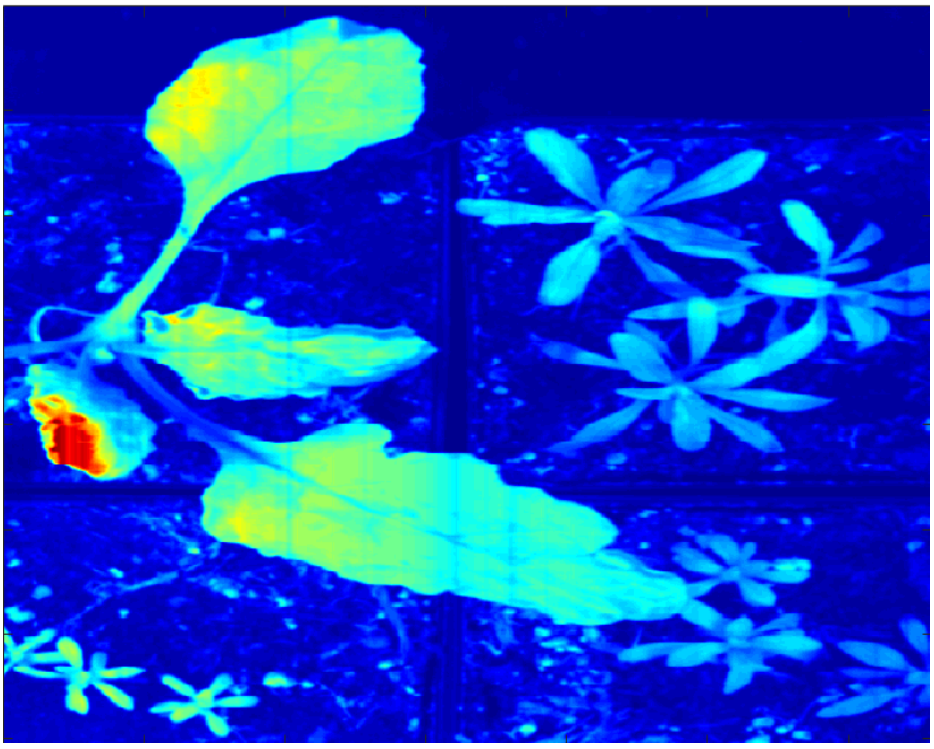

Figure B9. Visualization of false color image of calibrated image.

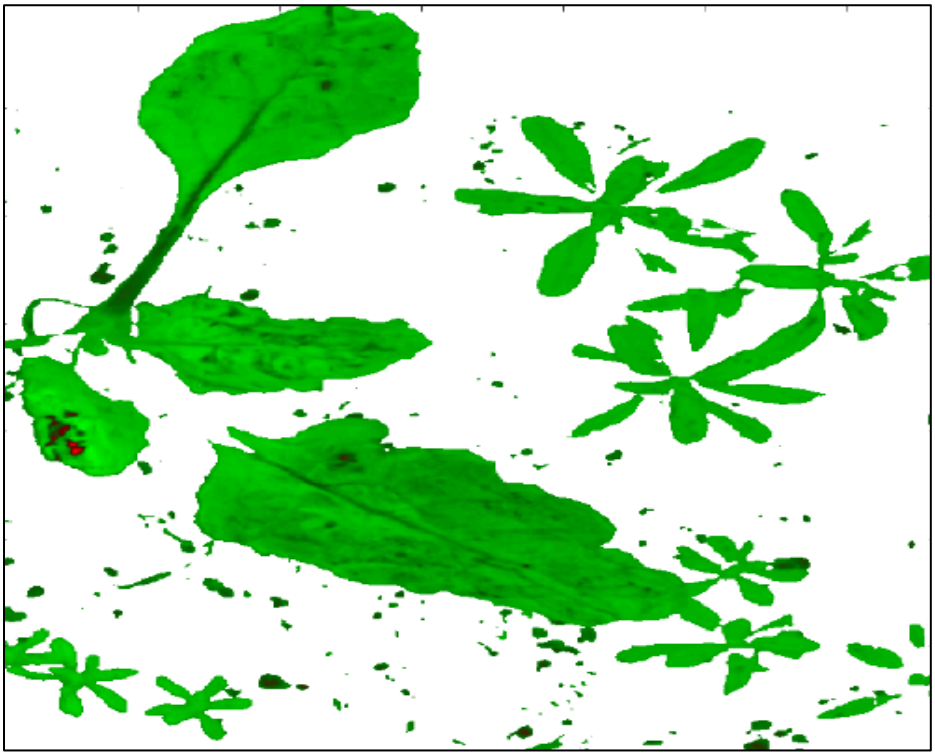

Figure B10. Soil background removed to help extract spectra values for kochia and sugarbeet.